

# Quantum Monte Carlo simulation of many-body dynamics with mitigated error on noisy quantum computer

Yongdan Yang,<sup>1</sup> Bing-Nan Lu,<sup>1</sup> and Ying Li<sup>1,\*</sup>

<sup>1</sup>*Graduate School of China Academy of Engineering Physics, Beijing 100193, China*

Quantum Monte Carlo and quantum simulation are both important tools for understanding quantum many-body systems. As a classical algorithm, quantum Monte Carlo suffers from the sign problem, preventing its applications to most fermion systems and real-time dynamics. In contrast, on a quantum computer, we can simulate time evolution of general systems with local interactions, yet such algorithms usually require the development of fault-tolerant quantum technologies. In this paper, we introduce a novel non-variational algorithm using quantum computing as a subroutine to accelerate quantum Monte Carlo. On a fault-tolerant quantum computer, the complexity of our algorithm is polynomial as the same as conventional quantum simulation algorithms. On a noisy quantum computer, our algorithm incorporating error mitigation eases the sign problem. Even when the circuit noise is significant, our algorithm can reduce the Monte Carlo variance by orders of magnitude.

## I. INTRODUCTION

Simulating quantum many-body systems is one of the main motivations for quantum computing [1]. A lot of quantum many-body problems are intractable in classical computing. An apparent reason is that the Hilbert space dimension increases exponentially with the system size, and storing the wavefunction of a large many-body system in classical memory is impossible. Quantum Monte Carlo (QMC) is a group of classical algorithms designed to bypass this memory issue. By sampling only the most important part of the configuration space, QMC can solve certain many-body problems at polynomial complexity, with the cost of introducing small statistical errors. Unfortunately, when applied to fermion systems, QMC encounters the notorious sign problem, which roots in the anti-symmetrisation nature of fermion wavefunctions. The sign problem means that the target amplitude is a highly-oscillating function with alternating sign, resulting in a variance increasing exponentially in the Monte Carlo simulation. A similar sign problem exists in simulating real-time dynamics. On the other hand, in quantum computing, by mapping the target wavefunction of the simulated system into the wavefunction of qubits, we can reproduce the dynamics of quantum systems while the memory and runtime scale polynomially [2]. In this paper, we establish the framework of quantum-circuit Monte Carlo (QCMC) algorithm, in which quantum computing is a subroutine of QMC. We show that this algorithm has a quantum advantage in solving many-body problems even on noisy quantum computers without fault tolerance.

Since Ulam and Metropolis's pioneer work of using random sampling to simulate real physical systems [3], the Monte Carlo method has grown into a large family of algorithms. Here we focus on a specific subset of Monte Carlo algorithms, namely, the QMC methods that are

based on real or imaginary time evolution [4–11]. These methods include Green's function Monte Carlo [11–13], auxiliary field Monte Carlo [14–16], world-line Monte Carlo [17–20] and their various variants. In what follows, we use pQMC to denote this set of algorithms. The other QMC algorithms are based on variational methods [21], and their connection to quantum computing is also an interesting topic, but will not be covered in this work.

In most pQMC methods we sample the configurations according to a quasi-probability amplitude derived from time evolution. For fermion systems such an amplitude is usually a complex number, which can be positive definite if the system respects certain symmetries. Examples of the latter case include half-filled Hubbard model with particle-hole exchange symmetry [22, 23] and nuclear system with Wigner-SU(4) symmetry [24–26]. However, a realistic Hamiltonian usually contains terms that break these symmetries and induce oscillating phases in the probability amplitude. As a result, even though pQMC methods are very successful in describing certain strongly correlated systems in chemistry [4, 5], condensed matter physics [6–10] and nuclear physics [11], its application is still rather limited due to the sign problem. Although in some important cases the sign problem can be alleviated using complicated techniques [27], e.g. complex Langevin method [28, 29] or Lefschetz thimble method [30–32], we can not find a generic solution as it is proven that the sign problem is NP-hard [33].

In quantum computing, the qubit and time costs for simulating the unitary time evolution of a quantum system scale polynomially with problem parameters, i.e. system size, evolution time and accuracy. Such algorithms include the Lie-Trotter-Suzuki decomposition [2, 34, 35], truncated Taylor series [36, 37], linear combinations of Lie-Trotter-Suzuki products [38, 39] and random compiler [40]. Based on the simulation of unitary time evolution, we can also simulate open-system dynamics [41–45], solve equilibrium-state problems [46–50] and find the ground state for certain Hamiltonians [51–57]. However, implementing these algorithms at a meaningful scale usu-

\* [yli@gscap.ac.cn](mailto:yli@gscap.ac.cn)

ally requires a fault-tolerant quantum computer [58–60], on which the logical error rate can be reduced to any level at a polynomial cost in quantum error correction [61]. In recent years, hybrid quantum-classical algorithms have been developed for applications before the era of fault-tolerant technologies [62], such as variational quantum algorithms for solving ground-state energy [63, 64], real-time simulation [65–69] and imaginary-time simulation [70, 71].

In this paper, we propose a hybrid non-variational quantum simulation algorithm, i.e. the QCMC algorithm. Contrary to the pQMC methods, there is no sign problem in simulating the time evolution using quantum computing. If we can delegate the calculation of the most oscillating part to quantum computing, the remaining calculations in pQMC might have a very mild sign problem or even free from it. To explore this possibility, the QCMC simulation is carried out by sampling random quantum circuits. We discuss several aspects of this hybrid scheme, including implementation of the time evolution operators, the total computational complexity, the optimal sampling distribution in Monte Carlo and the error-mitigation techniques. We show that our algorithm is polynomial on a fault-tolerant quantum computer and can reduce the variance of the Monte Carlo estimator even on a noisy quantum computer. Using quantum computing as a subroutine of pQMC, the circuit depth can be drastically reduced. Therefore, our algorithm is applicable to near-term noisy quantum hardware.

In the QCMC algorithm, we simulate many-body dynamics by expressing the time evolution operator in a summation form, and each term in the summation corresponds to a quantum circuit configuration. The summation formula is chosen to minimise the circuit depth and variance of the Monte Carlo estimator. We introduce two series of summation formulas based on Lie-Trotter-Suzuki product formulas [72, 73]: Pauli-operator-expansion (POE) formulas and leading-order-rotation (LOR) formulas. Compared with product formulas, the algorithmic error converges faster with the time step size  $\Delta t$  in our formulas at the cost of a moderately increased circuit depth: The second-order LOR formula converges as  $O(\Delta t^6)$ , which is even faster than the fourth-order product formula.

We mitigate errors in QCMC in three ways. First, our summation formulas are exact formulas of the time evolution operator for any finite time step size. The algorithmic error in QCMC is only due to the variance of the Monte Carlo estimator. This property of summation formulas allows us to take a large time step size and use shallow circuits to implement QCMC on a noisy quantum computer. Second, we use quantum error mitigation techniques to eliminate the impact of machine errors caused by noise in the quantum computer [65, 74, 75]. We present two types of circuits: Forward-backward circuits have larger depths than compact circuits but provide inherent error mitigation. Alternatively, probabilistic error cancellation is a universal way to mitigate machine

errors, which enlarges the estimator variance by a factor depending on the circuit depth [74, 76]. Considering probabilistic error cancellation applied to compact circuits, we can estimate the overall variance of QCMC due to both QMC and error mitigation. Third, we minimise the variance, i.e. the statistical error, by taking the optimal time step size. We obtain the minimised variance of QCMC in the form  $\sim e^{4\gamma h_{\text{tot}} t}$ , where  $\gamma$  is the increasing rate of the variance,  $h_{\text{tot}}$  characterises the magnitude of the Hamiltonian, and  $t$  is the evolution time.

QCMC has a variance depending on the error rate and achieves a quantum advantage even when the error rate is finite. For the second-order LOR formula, the variance increases at the rate of  $\gamma \simeq 2.45\epsilon^{0.82}$ , where  $\epsilon$  is the total gate error rate of one elementary Lie-Trotter-Suzuki product. QCMC is polynomial on a fault-tolerant quantum computer, because we can suppress  $\epsilon$  to any small value at a polynomial cost in quantum error correction. Suppose the variance in classical algorithms is in the same exponential form with a finite increasing rate  $\gamma_c$  [33], the quantum algorithm surpasses classical algorithms given an error rate of  $\epsilon \lesssim (\gamma_c/2.45)^{1/0.82}$ . As an example, the variance increasing rate in Green’s function Monte Carlo taking the computational basis is  $\gamma_c = 1$  for a large class of qubit Hamiltonians. Compared with this classical algorithm, QCMC reduces the variance by orders of magnitude even on a quantum computer with significant noise, e.g. by a factor of  $\sim 4 \times 10^4$  when  $h_{\text{tot}} t = 4$  and  $\epsilon = 0.1$ . As a result, the sample number required in Monte Carlo is reduced by the same factor.

This paper is organised as follows. In Sec. II, we briefly review Green’s function Monte Carlo and auxiliary-field Monte Carlo. In Sec. III, we sketch the QCMC algorithm. Two series of summation formulas are introduced in Sec. IV. Details of the QCMC algorithm are presented in the form of pseudocode in Sec. V. In Sec. VI, we give two types of quantum circuits (i.e. compact circuits and forward-backward circuits) for evaluating transition amplitudes. In Sec. VII, we discuss the optimal distribution for generating samples in Monte Carlo. Two quantum error mitigation protocols respectively using probabilistic error cancellation and forward-backward circuits are discussed in Sec. VIII. The QCMC algorithm and classical QMC algorithm are compared in Sec. IX. In Sec. X, we summarise the conclusions.

## II. QUANTUM MONTE CARLO

Many applications of pQMC can be formalised as computing the transition amplitude  $\langle \psi_f | e^{iH^*t} O e^{-iHt} | \psi_i \rangle$  given the initial state  $|\psi_i\rangle$ , final state  $|\psi_f\rangle$  and operator  $O$ . Here,  $H$  is the Hamiltonian, and  $t$  is a real or imaginary evolution time. A canonical approach is Green’s function Monte Carlo [11–13], in which the transition amplitude

is expressed in the path-integral form

$$\begin{aligned} & \langle \psi_f | e^{iHt^*} O e^{-iHt} | \psi_i \rangle \\ &= \int_{\mathbf{r}_0, \dots, \mathbf{r}_N, \mathbf{r}'_0, \dots, \mathbf{r}'_N} d\mathbf{r}_0 \cdots d\mathbf{r}_N d\mathbf{r}'_0 \cdots d\mathbf{r}'_N \\ & \quad \langle \psi_f | \mathbf{r}'_0 \rangle \langle \mathbf{r}'_0 | e^{iH \frac{t^*}{N}} | \mathbf{r}'_1 \rangle \cdots \langle \mathbf{r}'_{N-1} | e^{iH \frac{t^*}{N}} | \mathbf{r}'_N \rangle \langle \mathbf{r}'_N | O | \mathbf{r}_N \rangle \\ & \quad \times \langle \mathbf{r}_N | e^{-iH \frac{t}{N}} | \mathbf{r}_{N-1} \rangle \cdots \langle \mathbf{r}_1 | e^{-iH \frac{t}{N}} | \mathbf{r}_0 \rangle \langle \mathbf{r}_0 | \psi_i \rangle, \quad (1) \end{aligned}$$

where  $\{|\mathbf{r}\rangle\}$  is an orthonormal basis of the Hilbert space, and  $N$  is the number of time steps. The path integral is performed numerically using Monte Carlo methods.

Auxiliary-field Monte Carlo is another important approach of pQMC [14–16], which is characterized by the decomposition of particle-particle interactions into interactions of particles with a group of auxiliary fields, i.e.

$$e^{-iH\Delta t} \simeq \int ds A(s, \Delta t). \quad (2)$$

Here,  $A(s, \Delta t)$  is an operator depending on the auxiliary field  $s$ . Then, the transition amplitude is expressed as

$$\begin{aligned} & \langle \psi_f | e^{iHt^*} O e^{-iHt} | \psi_i \rangle \\ &= \int ds_1 \cdots ds_N ds'_1 \cdots ds'_N \langle \psi_f | A(s'_1, -\Delta t^*) \cdots \\ & \quad \times A(s'_N, -\Delta t^*) O A(s_N, \Delta t) \cdots A(s_1, \Delta t) | \psi_i \rangle. \quad (3) \end{aligned}$$

The operator  $A(s, \Delta t)$  is chosen such that  $\langle \psi_f | \cdots | \psi_i \rangle$  in the integral can be evaluated on a classical computer.

It often occurs that the amplitude  $q = \langle \psi_f | \cdots | \psi_i \rangle$  as a function of  $\mathbf{r}$  in Eq. (1) or as a function of  $s$  in Eq. (3) is not positive definite. In this case, we have to use the reweighting procedure by splitting  $q$  into its modulus and phase, i.e.  $q = |q|e^{i\theta_q}$ , and sample according to a probability distribution  $P \propto |q|$ . The expectation value of the remaining phase  $\langle e^{i\theta_q} \rangle$  indicates the degree of sign problem, and if it is much smaller than 1 then the sign problem is severe. In many pQMC simulations, this phase goes to zero exponentially for large system volume or particle number, which signifies very bad sign problem.

In some special cases, the sign problem is only induced by part of the integral variables. In other words, the amplitude  $q$  is a highly oscillating function of some variables and smooth function of the others. This usually occurs when the system is protected by an approximate symmetry. For example, for fermion systems with equal number of up and down spins, a spin-independent attractive interaction respecting the SU(2) spin symmetry will not induce the sign problem. In more general problems, the realistic interaction might be dominated by such a “good” component, while other “bad” components play a minor role but induce most of the sign problem. A typical example is the nuclear force, which is approximately independent of spin and isospin at low energy [26]. The spin-isospin dependent components and Coulomb force only contribute a small portion of the total nuclear binding energy, but introduce strong sign problem in the auxiliary field Monte Carlo calculations. Usually these inter-

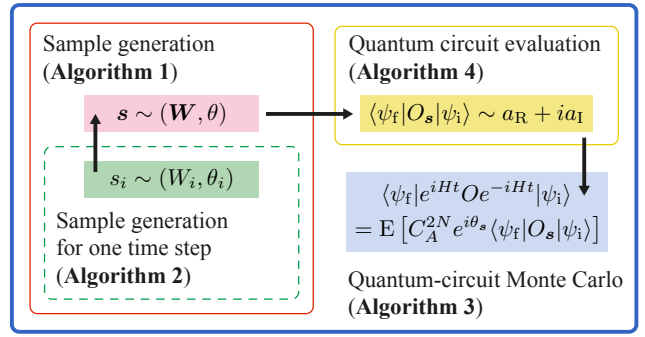


FIG. 1. Schematic diagram of the quantum-circuit Monte Carlo algorithm. The quantum computer evaluates  $\langle \psi_f | O_s | \psi_i \rangle$  according to samples  $s$  generated by the classical computer. The final estimate of the transition amplitude  $\langle \psi_f | e^{iHt} O e^{-iHt} | \psi_i \rangle$  is the empirical mean of results from the quantum computer up to a factor.

actions can be simulated using coupling constant extrapolation method [77] or perturbation theory [78], with the cost of additional uncertainties.

The above problem has an alternative solution in the quantum computing era. As a quantum computer can calculate the amplitude  $q$  with the same complexity regardless of the form of the interaction, we can use the quantum computer to simulate interactions causing the sign problem, while leave the smooth high-dimensional integrals to the classical Monte Carlo solver. For example, in the auxiliary-field Monte Carlo simulation of atomic nuclei [16], we can simulate the repulsive Coulomb force using quantum computing. In this paper, we introduce such a hybrid simulation scheme and establish a general framework for future works in this direction.

### III. QUANTUM-CIRCUIT MONTE CARLO

To implement QMC using a quantum computer, we replace the integral over the auxiliary field with a summation over unitary operators. The time evolution operator is expressed in the summation form

$$e^{-iH\Delta t} = \sum_s c(s) U(s), \quad (4)$$

where  $U(s)$  are unitary operators, and  $c(s)$  are complex coefficients. For real time evolution, approximate summation formulas have been proposed, including truncated Taylor expansion [36, 37] and linear combinations of Lie-Trotter-Suzuki products [38, 39]. In this paper, we propose exact summation formulas of the time evolution operator (see Sec. IV). By combining quantum circuits and the Monte Carlo method, our exact formulas can be implemented for any finite time step size  $\Delta t$ . In quantum circuits, the gate number of each time step is only moderately increased upon the Lie-Trotter-Suzuki product (see

Sec. VI), and we can minimise the number of time steps  $N$  by maximising  $\Delta t$ . Because of the minimised circuit depth, which is proportional to  $N$ , our formulas are practical on noisy quantum computer without fault tolerance.

With the summation expression of the time evolution operator, the transition amplitude in the path-integral form becomes

$$\langle \psi_f | e^{iHt} O e^{-iHt} | \psi_i \rangle = \sum_{s_1, \dots, s_N, s'_1, \dots, s'_N} \left( \prod_{i=1}^N c(s_i) c(s'_i)^* \right) \langle \psi_f | O_s | \psi_i \rangle \quad (5)$$

where  $\mathbf{s} = (s_1, \dots, s_N, s'_1, \dots, s'_N)$  and

$$O_s = U(s'_1)^\dagger \cdots U(s'_N)^\dagger O U(s_N) \cdots U(s_1). \quad (6)$$

In this paper, we focus on real time evolution. With real time evolution, we can construct quantum phase estimation circuits [53, 54, 56], eigenenergy filtering operators [55, 57] and imaginary time evolution operators for solving eigenstate and finite-temperature problems. One can realise a summation formula by either using a deterministic circuit [36–38] or sampling random circuits [39, 40]. To minimise the circuit depth, we compute the transition amplitude using random circuits: We sample random unitary operators (i.e. the parameter  $\mathbf{s}$ ) on the classical computer, evaluate  $\langle \psi_f | O_s | \psi_i \rangle$  on the quantum computer and then compute the path-integral summation using the Monte Carlo method on the classical computer. See Fig. 1 for a schematic diagram of the QCML algorithm and Sec. V for details.

Without fault tolerance, we use error mitigation techniques to eliminate errors in quantum circuits. In the quantum error mitigation based on quasi-probability decomposition (i.e. probabilistic error cancellation) [74, 76], each unitary circuit for evaluating  $\langle \psi_f | O_s | \psi_i \rangle$  is decomposed into a linear combination of noisy circuits. Then, the overall algorithm includes Monte Carlo summations over unitary operators and also noisy circuits. Details of the error mitigation are given in Sec. VIII. Using our exact formulas of the time evolution operator and assuming that quasi-probability decompositions are also exact, the sampling noise in Monte Carlo is the only source of error in our algorithm.

### Sampling noise and normalisation factor

The Monte Carlo summation has a finite variance depending on the sampling approach. To compute the transition amplitude in Eq. (5), we randomly generate samples of  $\mathbf{s}$  with a probability distribution  $P(\mathbf{s})$ . According to the importance sampling, the variance is minimised by taking the optimal distribution

$$P(\mathbf{s}) \propto \left| \left( \prod_{i=1}^N c(s_i) c(s'_i)^* \right) \langle \psi_f | O_s | \psi_i \rangle \right|.$$

Implementing the optimal distribution requires the knowledge of  $|\langle \psi_f | O_s | \psi_i \rangle|$ .

In this paper, we focus on a practical suboptimal distribution

$$P(\mathbf{s}) = \left| \prod_{i=1}^N c(s_i) c(s'_i)^* \right| / C_A^{2N}, \quad (7)$$

where the normalisation factor  $C_A = \sum_s |c(s)|$  determines the variance. Taking the suboptimal distribution, the transition amplitude  $\langle \psi_f | e^{iHt} O e^{-iHt} | \psi_i \rangle$  is the expected value of  $C_A^{2N} e^{i\theta_s} \langle \psi_f | O_s | \psi_i \rangle$ , where

$$\theta_s = \arg \left( \prod_{i=1}^N c(s_i) c(s'_i)^* \right). \quad (8)$$

Formally, we have

$$\langle \psi_f | e^{iHt} O e^{-iHt} | \psi_i \rangle = E [C_A^{2N} e^{i\theta_s} \langle \psi_f | O_s | \psi_i \rangle] = \sum_s P(\mathbf{s}) C_A^{2N} e^{i\theta_s} \langle \psi_f | O_s | \psi_i \rangle. \quad (9)$$

Taking the suboptimal distribution, the estimator of  $\langle \psi_f | e^{iHt} O e^{-iHt} | \psi_i \rangle$  is

$$\hat{A} = C_A^{2N} \langle e^{i\theta_s} \langle \psi_f | O_s | \psi_i \rangle \rangle_{N_s}. \quad (10)$$

Here,  $\langle \bullet \rangle_{N_s}$  denotes the empirical mean taken over  $N_s$  samples of  $\mathbf{s}$ . The variance of the estimator is

$$\text{Var}(\hat{A}) = \frac{1}{N_s} C_A^{4N} \text{Var}(e^{i\theta_s} \langle \psi_f | O_s | \psi_i \rangle). \quad (11)$$

When  $O$  is a unitary operator,  $|\langle \psi_f | O_s | \psi_i \rangle| \leq 1$ , and the variance has the upper bound

$$\text{Var}(\hat{A}) \leq \frac{1}{N_s} C_A^{4N}. \quad (12)$$

In our QCML algorithm, we use circuits given in Sec. VI to evaluate  $\langle \psi_f | O_s | \psi_i \rangle$ . Each quantum circuit reports a probabilistic binary outcome, whose expected value is either the real or imaginary part of  $e^{i\theta_s} \langle \psi_f | O_s | \psi_i \rangle$ . We find that the suboptimal distribution (which is suboptimal when we can deterministically evaluate  $\langle \psi_f | O_s | \psi_i \rangle$ ) is actually the optimal distribution for the probabilistic evaluation without prior knowledge of  $|\langle \psi_f | O_s | \psi_i \rangle|$ , see VII. Accordingly, the minimum variance is

$$\text{Var}(\hat{A}) = \frac{1}{M_{\text{tot}}} \left( 2C_A^{4N} - |\langle \psi_f | e^{iHt} O e^{-iHt} | \psi_i \rangle|^2 \right), \quad (13)$$

where  $2M_{\text{tot}}$  is the total number of quantum circuit shots, and each shot is an implementation of the circuit that returns one binary measurement outcome.

We can find that ideally  $C_A = 1$ , i.e. the variance does not increase with the number of time steps. This limit can be approached on a fault-tolerant quantum computer: We take a sufficiently small  $\Delta t$ ,  $c(1) \simeq 1$ ,  $U(1) \simeq e^{-iH\Delta t}$  is a Lie-Trotter-Suzuki product, and terms with  $s > 1$  are negligible. On a noisy quantum computer,  $C_A$  is always greater than one. A large part of our effort is devoted to minimising  $C_A$ , in order to reduce the variance.

#### IV. SUMMATION FORMULAS OF TIME EVOLUTION OPERATORS

We look for summation formulas satisfying the following criteria:

- Unitary operators  $U(s)$  are easy to be implemented using elementary quantum gates, for reducing the gate number;
- The normalisation factor  $C_A$  is minimised;
- Samples of  $s$  can be efficiently generated on a classical computer according to the distribution in Eq. (7).

We propose two types of summation formulas in this paper as examples of the general approach. By adding Pauli operators to Lie-Trotter-Suzuki products, we obtain POE formulas. For an  $l$ th-order product formula, the corresponding POE summation formula has the normalisation factor  $C_A = 1 + O(\Delta t^{l+1})$ . By replacing leading-order Pauli operators with rotation operators, we obtain LOR formulas, and the normalisation factor is reduced to  $C_A = 1 + O(\Delta t^{2l+2})$ .

In the following, we first discuss Lie-Trotter-Suzuki product formulas and then introduce our summation formulas.

##### A. Product formulas

In this section, we review Lie-Trotter-Suzuki product formulas [72, 73] and discuss some properties important for our discussion. Given the Hamiltonian  $H = \sum_{j=1}^M H_j$ , where  $H_j$  are Hermitian operators, the first-order formula reads

$$S_1(\Delta t) = e^{-iH_M \Delta t} \cdots e^{-iH_1 \Delta t} = e^{-iH \Delta t} + O(\Delta t^2). \quad (14)$$

Higher-order formulas are defined recursively for any positive integer  $m$  by

$$\begin{aligned} S_{2m}(\Delta t) &= K_{2m}(-\Delta t)^\dagger K_{2m}(\Delta t) \\ &= e^{-iH \Delta t} + O(\Delta t^{2m+1}), \end{aligned} \quad (15)$$

where  $K_2(\Delta t) = S_1(\frac{\Delta t}{2})$ ,

$$K_{2m}(\Delta t) = K_{2m-2}((1 - 2rp_{r,m})\Delta t) S_{2m-2}(p_{r,m}\Delta t)^r \quad (16)$$

when  $m > 1$ , and  $p_{r,m} = \left[2r - (2r)^{\frac{1}{2m+1}}\right]^{-1}$ . Here,  $r$  can be any positive integer. We can find that each  $S_{2m}$  is a product of  $2r + 1$   $S_{2m-2}$  operators.

For the first-order formula, we define the correction operator

$$V_1(\Delta t) \equiv e^{-iH \Delta t} S_1(\Delta t)^\dagger = e^{-i \sum_{k=2}^{\infty} R_1^{(k)} \Delta t^k}, \quad (17)$$

where  $R_1^{(k)}$  are operators independent of  $\Delta t$ . Because  $V_1(\Delta t)$  is unitary for all real  $\Delta t$ , all  $R_1^{(k)}$  are Hermitian operators. Then,

$$V_1(\Delta t) = \mathbb{1} - iL_1(\Delta t) + O(\Delta t^4), \quad (18)$$

where the leading-order operator

$$L_1(\Delta t) = R_1^{(2)} \Delta t^2 + R_1^{(3)} \Delta t^3 \quad (19)$$

is Hermitian. Later, we will show that the Hermitian leading-order operator is important for minimising the normalisation factor  $C_A$ .

For higher-order formulas, correction operators are

$$\begin{aligned} V_{2m}(\Delta t) &\equiv K_{2m}(-\Delta t) e^{-iH \Delta t} K_{2m}(\Delta t)^\dagger \\ &= e^{-i \sum_{k=2m+1}^{\infty} R_{2m}^{(k)} \Delta t^k}, \end{aligned} \quad (20)$$

where  $R_{2m}^{(k)}$  are Hermitian operators independent of  $\Delta t$ . Because of the symmetric form,  $V_{2m}(\Delta t) = V_{2m}(-\Delta t)^\dagger$  for all real  $\Delta t$ , and  $R_{2m}^{(k)} = 0$  for all even  $k$  []. Then,

$$V_{2m}(\Delta t) = \mathbb{1} - iL_{2m}(\Delta t) + O(\Delta t^{4m+2}), \quad (21)$$

where the leading-order operator

$$L_{2m}(\Delta t) = \sum_{k=m}^{2m} R_{2m}^{(2k+1)} \Delta t^{2k+1} \quad (22)$$

is Hermitian. For the second-order formula,

$$L_2(\Delta t) = R_2^{(3)} \Delta t^3 + R_2^{(5)} \Delta t^5. \quad (23)$$

##### B. Summation formulas

To simplify quantum circuits, we work with Pauli operators  $\mathbf{P}_n = \{I, X, Y, Z\}^{\otimes n}$  as the basis of matrix space, where  $n$  is the number of qubits. Without loss of generality, we assume that each term of the Hamiltonian is a Pauli operator, i.e.  $H_j = h_j \sigma_j$ , where  $\sigma_j \in \mathbf{P}_n$ , and  $h_j$  is a real coefficient. We define  $h_{\text{tot}} \equiv \sum_j |h_j|$  which characterises the magnitude of the Hamiltonian.

Given the time evolution operator, there exist many different summation formulas  $e^{-iH \Delta t} = \sum_s c(s) U(s)$ . Each formula represents a sampling protocol in Monte Carlo. For example,

$$e^{-iH \Delta t} = \sum_{\sigma \in \mathbf{P}_n} 2^{-n} \text{Tr}(\sigma e^{-iH \Delta t}) \sigma. \quad (24)$$

Such a formula is impractical, because computing coefficients  $\text{Tr}(\sigma e^{-iH \Delta t})$  on a classical computer is usually difficult when  $n$  is large.

For the practical implementation, we express the time evolution operator in the form

$$e^{-iH \Delta t} = K_L V K_R, \quad (25)$$

where  $K_L$  and  $K_R$  are unitary operators in the Lie-Trotter-Suzuki product form, and  $V$  is the correction operator, see Eqs. (17) and (20). We apply the Taylor expansion to the correction operator to obtain the summation formula. We divide the Taylor expansion into three parts,  $V = \mathbb{1} - iL + T$ , where  $L$  is the leading-order operator, and  $T$  is the high-order operator. The normalisation factor of a POE summation formula is  $C_A = 1 + C_L + C_T$ ,

Pauli-operator-expansion formulas	$C_A = 1 + C_L + C_T$			
Leading-order-rotation formulas	$C_A = \sqrt{1 + C_L^2} + C_T$			
High-order contribution $C_T$	$e^{\lambda x} - \sum_{k=0}^{2l+1} \frac{1}{k!} (\lambda x)^k$			
$l$ (order of formula)	0	1	2	$2m$
$\lambda$	1	2	2	$1 + \prod_{k=2}^m (4rp_{r,k} - 1)$
Leading-order contribution $C_L$	$x$	$\frac{1}{2}(2x)^2 + \frac{1}{6}(2x)^3$	$\frac{1}{6}(2x)^3 + \frac{1}{120}(2x)^5$	$\sum_{k=m}^{2m} \frac{1}{(2k+1)!} (\lambda x)^{2k+1}$
Simplified leading-order contribution $C_L$	$< \frac{1}{2}x^2 + \frac{1}{6}(2x)^3$	$< \frac{1}{18}x^3 + \frac{1}{120}(2x)^5$		

TABLE I. Normalisation factors of summation formulas. In the table,  $x \equiv h_{\text{tot}}\Delta t$ .

where  $C_L$  and  $C_T$  are contributions of  $L$  and  $T$ , respectively. The normalisation factor of a LOR summation formula is  $C_A = \sqrt{1 + C_L^2} + C_T$ . Normalisation factors of all the formulas are summarised in Table I.

### 1. Zeroth-order Pauli-operator-expansion formula

The direct Taylor expansion of the time evolution operator gives the zeroth-order summation formula

$$V_0(\Delta t) = e^{-iH\Delta t} = \mathbb{1} - iL_0(\Delta t) + T_0(\Delta t), \quad (26)$$

where the Hermitian leading-order operator is

$$L_0(\Delta t) = \sum_j h_j \Delta t \sigma_j, \quad (27)$$

and the high-order operator is

$$T_0(\Delta t) = \sum_{k=2}^{\infty} \sum_{j_1, \dots, j_k=1}^M \frac{\prod_{a=1}^k (-ih_{j_a} \Delta t)}{k!} \sigma_{j_k} \cdots \sigma_{j_1}. \quad (28)$$

The normalisation factor is given by  $C_L = h_{\text{tot}}\Delta t$  and  $C_T = e^{h_{\text{tot}}\Delta t} - (1 + h_{\text{tot}}\Delta t)$ .

### 2. First-order Pauli-operator-expansion formula

According to the first-order product formula, we express the time evolution operator as

$$e^{-iH\Delta t} = V_1(\Delta t)S_1(\Delta t). \quad (29)$$

We obtain the summation formula by applying the Taylor expansion to each exponential in the correction operator,

$$\begin{aligned} V_1(\Delta t) &= e^{-iH\Delta t} e^{ih_1 \sigma_1 \Delta t} \cdots e^{ih_M \sigma_M \Delta t} \\ &= \mathbb{1} - iL_1(\Delta t) + T_1(\Delta t), \end{aligned} \quad (30)$$

where

$$L_1(\Delta t) = iF_1^{(2)}(\Delta t) + iF_1^{(3)}(\Delta t), \quad (31)$$

$$T_1(\Delta t) = \sum_{k=4}^{\infty} F_1^{(k)}(\Delta t), \quad (32)$$

and

$$\begin{aligned} F_1^{(k')}(\Delta t) &= \sum_{k, k_1, \dots, k_M=0}^{\infty} \sum_{j_1, \dots, j_k=1}^M \delta_{k', k + \sum_{j=1}^M k_j} \\ &\quad \times \frac{\prod_{a=1}^k (-ih_{j_a} \Delta t)}{k!} \left[ \prod_{j=1}^M \frac{(ih_j \Delta t)^{k_j}}{k_j!} \right] \\ &\quad \times \sigma_{j_k} \cdots \sigma_{j_1} \sigma_1^{k_1} \cdots \sigma_M^{k_M}. \end{aligned} \quad (33)$$

Note that the first term in  $L_1$  is  $O(\Delta t^2)$  according to discussions on product formulas. For the first-order formula, the normalisation factor is given by  $C_L = \frac{1}{2}(2h_{\text{tot}}\Delta t)^2 + \frac{1}{6}(2h_{\text{tot}}\Delta t)^3$  and  $C_T = e^{2h_{\text{tot}}\Delta t} - \sum_{k=0}^3 \frac{1}{k!} (2h_{\text{tot}}\Delta t)^k$ .

### 3. Second-order Pauli-operator-expansion formula

Similar to the first-order formula, according to the second-order product formula, we express the time evolution operator as

$$e^{-iH\Delta t} = S_1\left(-\frac{\Delta t}{2}\right)^\dagger V_2(\Delta t) S_1\left(\frac{\Delta t}{2}\right). \quad (34)$$

The Taylor expansion of the correction operator reads

$$V_2(\Delta t) = \mathbb{1} - iL_2(\Delta t) + T_2(\Delta t), \quad (35)$$

where

$$L_2(\Delta t) = iF_2^{(3)}(\Delta t) + iF_2^{(5)}(\Delta t), \quad (36)$$

$$T_2(\Delta t) = \sum_{k=6}^{\infty} F_2^{(k)}(\Delta t), \quad (37)$$

and

$$\begin{aligned} F_2^{(k')}(\Delta t) &= \sum_{k, k_1, \dots, k_M=0}^{\infty} \sum_{j_1, \dots, j_k=1}^M \delta_{k', k + \sum_{j=1}^M (k_j + k'_j)} \\ &\quad \times \frac{\prod_{a=1}^k (-ih_{j_a} \Delta t)}{k!} \left[ \prod_{j=1}^M \frac{(ih_j \Delta t/2)^{k_j + k'_j}}{k_j! k'_j!} \right] \\ &\quad \times \sigma_M^{k'_M} \cdots \sigma_1^{k'_1} \sigma_{j_k} \cdots \sigma_{j_1} \sigma_1^{k_1} \cdots \sigma_M^{k_M}. \end{aligned} \quad (38)$$

According to discussions on product formulas,  $L_2$  only contain  $\Delta t^3$  and  $\Delta t^5$  terms. For the second-order formula, the normalisation factor is given by  $C_L = \frac{1}{6}(2h_{\text{tot}}\Delta t)^3 + \frac{1}{120}(2h_{\text{tot}}\Delta t)^5$  and  $C_T = e^{2h_{\text{tot}}\Delta t} - \sum_{k=0}^5 \frac{1}{k!}(2h_{\text{tot}}\Delta t)^k$ .

#### 4. Higher-order Pauli-operator-expansion formulas

For the  $2m$ th-order formula, we express the time evolution operator as

$$e^{-iH\Delta t} = K_{2m}(-\Delta t)^\dagger V_2(\Delta t) K_{2m}(\Delta t). \quad (39)$$

Then, we can obtain the POE summation formula by applying Taylor expansion to each exponential in the correction operator  $V_2$ , similar to the first-order and second-order formulas. The normalisation factor of the  $2m$ th-order formula is given by  $C_L = \sum_{k=m}^{2m} \frac{1}{(2k+1)!} (\lambda h_{\text{tot}}\Delta t)^{2k+1}$  and  $C_T = e^{\lambda h_{\text{tot}}\Delta t} - \sum_{k=0}^{4m+1} \frac{1}{k!} (\lambda h_{\text{tot}}\Delta t)^k$ . Here, the factor  $\lambda = 1 + \prod_{k=2}^m (4rp_{r,k} - 1)$  is due to the backward evolution with the time  $(1 - 2rp_{r,m})\Delta t$  in the product formula.

#### 5. Simplified leading-order operators

By combining terms with the same Pauli operator in the summation formula, we can reduce the normalisation factor. For example, if both  $\alpha\sigma$  and  $-\alpha\sigma$  exist in the summation formula, the contribution to the normalisation factor is  $2|\alpha|$ , which is reduced to zero after combining like terms. We apply this approach to  $F_1^{(2)}$  and  $F_2^{(3)}$  in  $L_1$  and  $L_2$ , respectively, to minimise the dominant contribution to the normalisation factor. See Appendix A for the simplified expressions of  $F_1^{(2)}$  and  $F_2^{(3)}$ . As a result, the leading-order contributions are reduced to  $C_L < \frac{1}{2}(h_{\text{tot}}\Delta t)^2 + \frac{1}{6}(2h_{\text{tot}}\Delta t)^3$  in the first-order formula and  $C_L < \frac{1}{18}(h_{\text{tot}}\Delta t)^2 + \frac{1}{120}(2h_{\text{tot}}\Delta t)^5$  in the second-order formula.

#### 6. Leading-order-rotation formulas

The leading-order operator  $L_l$  is Hermitian, which allows us to reduce its contribution to the normalisation factor  $C_A$  from  $O(\Delta t^{l+1})$  to  $O(\Delta t^{2l+2})$ . We suppose that the Pauli-operator summation form of  $L_l$  is

$$L_l = \sum_u \alpha_u \tau_u, \quad (40)$$

where  $\tau_u \in \mathbf{P}_n$  are Pauli operators. Here, all  $\alpha_u$  are real because  $L_l$  is Hermitian, which is the key of LOR formulas. To minimise the normalisation factor, we express leading-order terms as a summation of rotation operators,

$$\mathbb{1} - iL_l = \sum_u \beta_u e^{-i\text{sgn}(\alpha_u)\phi\tau_u}, \quad (41)$$

where  $\phi = \arctan(C_L)$ ,  $\beta_u = |\alpha_u|/\sin\phi$  and  $C_L = \sum_u |\alpha_u|$ .

The normalisation factor contributed by  $\mathbb{1} - iL_l$  is  $1 + C_L$  in POE formulas, which is reduced to  $\sum_i |\beta_u| = C_L/\sin\phi = \sqrt{1 + C_L^2} \simeq 1 + C_L^2/2$  in LOR formulas. Note that  $C_L = O(\Delta t^{l+1})$  and  $C_T = O(\Delta t^{2l+2})$ . By using LOR formulas, we reduce the normalisation factor  $C_A$  from  $1 + O(\Delta t^{l+1})$  to  $1 + O(\Delta t^{2l+2})$ .

We have introduced all of our summation formulas. We remark that our summation formulas are used for sampling random  $U(s)$  rather than sampling quantum operations [40], which corresponds to a summation of completely positive maps instead of operators.

### C. Comparison between formulas

Now, we compare different formulas of the time evolution operator in the fault-tolerant limit, i.e. gate errors are negligible. In this case, we can use deep quantum circuits to implement the formulas and take a sufficiently small time step size  $\Delta t$ . We leave the discussions on noisy quantum computing to Secs. VIII and IX.

When gate errors are negligible, sampling noise is the only source of error for our exact summation formulas. The error due to sampling noise is  $\sim \frac{1}{\sqrt{N_s}} C_A^{2N}$ . Therefore, the error for the  $l$ th-order POE formula is  $\sim \frac{1}{\sqrt{N_s}} + \frac{2N}{\sqrt{N_s}} O(\Delta t^{l+1})$ , and the error for the  $l$ th-order LOR formula is  $\sim \frac{1}{\sqrt{N_s}} + \frac{2N}{\sqrt{N_s}} O(\Delta t^{2l+2})$ .

For Lie-Trotter-Suzuki product formulas, there are two sources of error: The error due to finite  $\Delta t$ , i.e. the formulas are approximate, and the error due to sampling noise. The error due to finite  $\Delta t$  is systematic and cannot be reduced by increasing the number of samples. For the  $l$ -th order product formula, the error is  $\sim \frac{1}{\sqrt{N_s}} + NO(\Delta t^{l+1})$ , where the first term is due to the sampling noise, and the second term is due to the finite  $\Delta t$ . We note that on a fault-tolerant quantum computer, we can use amplitude amplification to accelerate the evaluation of an amplitude of the wavefunction [79]. Amplitude amplification can be applied to product formulas; how to apply it to our summation formulas is an open question.

We can find that for the same order of formulas, our summation formulas have a smaller error than product formulas, due to the factor  $\frac{1}{\sqrt{N_s}}$  in the  $\Delta t$  term and the increased exponent of  $\Delta t$  (for LOR formulas). The reduced error is at the cost of increased circuit depth: To implement our formulas, we need to add a correction operator to the Lie-Trotter-Suzuki product for each time step. A correction operator is either a Pauli operator  $\sigma$  or a rotation operator in the form  $e^{-i\phi\sigma}$ . In Sec. VIC, we show that implementing the correction operator for POE and LOR formulas require at most  $n$  and  $4n$  controlled-NOT gates, respectively, on an all-to-all qubit network ( $4n - 3$  and  $8n - 4$  gates, respectively, on a linear qubit network). Here  $n$  is the qubit number. Unless the Hamiltonian has the simplest structure, such as the one-dimensional quan-

tum Ising model, it is reasonable to assume that the gate number for the first-order Lie-Trotter-Suzuki product  $S_1$  is more than  $2n$ . Therefore, the circuit depth increase-  
ment is moderate.

The linear combination of Lie-Trotter-Suzuki products can efficiently reduce the error due to finite  $\Delta t$  [38, 39]. The simplest example is  $e^{-iH\Delta t} = \frac{4}{3}S_2(\Delta t/2)^2 - \frac{1}{3}S_2(\Delta t) + O(\Delta t^5)$ . We can find that the error for our second-order LOR formula converges faster as  $O(\Delta t^6)$ , and the circuit depth is smaller compared with  $S_2^2$  (assuming the depth for one  $S_2$  is larger than a correction operator).

## V. ALGORITHM

The algorithm consists of three phases. First, the classical computer generates samples of  $\mathbf{s}$  according to the distribution given by Eq. (7) and composes corresponding quantum circuits. Second, the quantum computer implements circuits to evaluate  $\langle \psi_f | O_s | \psi_i \rangle$ . Finally, with results from the quantum computer, the classical computer calculates the expected value of  $e^{i\theta_s} \langle \psi_f | O_s | \psi_i \rangle$  and returns the final estimate of the transition amplitude  $\langle \psi_f | e^{iHt} O e^{-iHt} | \psi_i \rangle$ .

In this section, we present the first and final phases of the algorithm, which are implemented on the classical computer. We leave details of the second phase, i.e. quantum computing, to the next section. We focus on second-order summation formulas, and algorithms for other summation formulas are similar.

### A. Sampling algorithm

The Hamiltonian is specified by a vector of real numbers  $\mathbf{h} = (h_1, \dots, h_M)$  and a vector of Pauli operators  $\boldsymbol{\sigma} = (\sigma_1, \dots, \sigma_M)$ . Given the evolution time  $t$ , we need to choose a number of time steps  $N$ , then the corresponding time step size is  $\Delta t = t/N$ . These parameters  $\mathbf{h}$ ,  $\boldsymbol{\sigma}$ ,  $N$  and  $\Delta t$  are inputs to the sampling algorithm. To present the algorithm in a way that works for both POE and LOR formulas, we introduce an additional input parameter  $F = P, R$  to denote POE and LOR formulas, respectively.

#### Algorithm 1 Sample generation.

---

```

1: function SAMGEN( $F, \mathbf{h}, \boldsymbol{\sigma}, N, \Delta t$ )
2:   for  $i = 1$  to  $N$  do
3:      $(W_i, \theta_i) \leftarrow \text{SAMGENONESTEP}(F, \mathbf{h}, \boldsymbol{\sigma}, \Delta t)$ 
4:      $(W'_i, \theta'_i) \leftarrow \text{SAMGENONESTEP}(F, \mathbf{h}, \boldsymbol{\sigma}, \Delta t)$ 
5:    $\mathbf{W} \leftarrow (W_1, \dots, W_N, W'_1, \dots, W'_N)$ 
6:    $\theta \leftarrow \sum_{i=1}^N (\theta_i - \theta'_i)$ 
7:   Output  $(\mathbf{W}, \theta)$ .

```

---

#### Algorithm 2 Sample generation for one time step.

---

```

1: function SAMGENONESTEP( $F, \mathbf{h}, \boldsymbol{\sigma}, \Delta t$ )
2:   Compute  $L_2$  according to Eq. (36), simplify  $L_2$  by
   combining like terms, obtain the final expression  $L_2 =$ 
    $\sum_u \alpha_u \tau_u$ .  $\triangleright \tau_u \in \mathbf{P}_n$ 
3:    $C_L \leftarrow \sum_u |\alpha_u|$ 
4:    $C_T \leftarrow e^{2h_{\text{tot}}\Delta t} - \sum_{k=0}^5 \frac{1}{k!} (2h_{\text{tot}}\Delta t)^k \triangleright h_{\text{tot}} = \sum_j |h_j|$ 
5:   if  $F = P$  then  $C_A \leftarrow 1 + C_L + C_T$ 
6:   else if  $F = R$  then  $C_A \leftarrow \sqrt{1 + C_L^2} + C_T$ 
7:   Choose  $O$  from  $L$  and  $T$  with probabilities  $(C_A - C_T)/C_A$  and  $C_T/C_A$ , respectively.
8:   if  $O = L$  then  $\triangleright$  Sample from leading-order terms
9:     if  $F = P$  then Choose  $(W, \theta)$  from  $(\mathbf{1}, 0)$  and
      $\{(\tau_u, \arg(-i\alpha_u))\}$  with probabilities  $1/(1 + C_L)$  and
      $\{|\alpha_u|/(1 + C_L)\}$ , respectively.
10:    else if  $F = R$  then Choose  $(W, \theta)$  from
      $\{e^{-i\text{sgn}(\alpha_u)\phi\tau_u}, 0\}$  with probabilities  $\{|\alpha_u|/C_L\}$ .
      $\triangleright \phi = \arctan(C_L)$ 
11:   else if  $O = T$  then  $\triangleright$  Sample from high-order terms
12:      $k, k_j, k'_j \leftarrow 0$ 
13:     while  $k + \sum_{j=1}^M (k_j + k'_j) < 6$  do
14:        $k \leftarrow \text{POISSON}(h_{\text{tot}}\Delta t)$   $\triangleright \text{POISSON}(x)$  returns
        $k \in \{0, 1, \dots\}$  with the probability  $e^{-x} x^k / k!$ .
15:       for  $j = 1$  to  $M$  do
16:          $k_j \leftarrow \text{POISSON}(|h_j| \Delta t / 2)$ 
17:          $k'_j \leftarrow \text{POISSON}(|h'_j| \Delta t / 2)$ 
18:       for  $a = 1$  to  $k$  do Choose  $j_a$  from  $\{1, \dots, M\}$  with
       probabilities  $\{|h_{j_a}| / h_{\text{tot}}\}$ .
19:        $W \leftarrow \zeta^* \sigma_M^{k'_M} \cdots \sigma_1^{k'_1} \sigma_{j_k} \cdots \sigma_{j_1} \sigma_1^{k_1} \cdots \sigma_M^{k_M}$ 
        $\triangleright$  Take  $\zeta = \pm 1, \pm i$  to meet  $W \in \mathbf{P}_n$ .
20:        $\theta \leftarrow \arg \left( \zeta \prod_{a=1}^k (-ih_{j_a}) \times \prod_{j=1}^M (ih_j)^{k_j + k'_j} \right)$ 
21:   Output  $(W, \theta)$ .

```

---

In second-order summation formulas, each term is in the form  $S_1(-\frac{\Delta t}{2})^\dagger W S_1(\frac{\Delta t}{2})$ : In the POE formula,  $W$  is always a Pauli operator; in the LOR formula,  $W$  is either a rotation operator or a Pauli operator. Taking  $U(s_i) = S_1(-\frac{\Delta t}{2})^\dagger W_i S_1(\frac{\Delta t}{2})$  and  $U(s'_i) = S_1(-\frac{\Delta t}{2})^\dagger W'_i S_1(\frac{\Delta t}{2})$ , we have

$$O_s = S_1^\dagger W_1'^\dagger S_1' \cdots S_1^\dagger W_N'^\dagger S_1' \cdots S_1' W_N S_1 \cdots S_1' W_1 S_1, \quad (42)$$

Here, we have used notations  $S_1 = S_1(\frac{\Delta t}{2})$  and  $S'_1 = S_1(-\frac{\Delta t}{2})^\dagger$  for simplicity. Given the vector of correction operators

$$\mathbf{W} = (W_1, \dots, W_N, W'_1, \dots, W'_N), \quad (43)$$

the quantum computer can evaluate  $\langle \psi_f | O_s | \psi_i \rangle$ .

In the final phase, the classical computer estimates the transition amplitude by computing the expected value of  $e^{i\theta_s} \langle \psi_f | O_s | \psi_i \rangle$ . Therefore, the sampling algorithm also needs to output  $\theta_s$ .

Overall, outputs of the sampling algorithm are  $\mathbf{W}$  and  $\theta$ . The procedure for generating  $\mathbf{W}$  and  $\theta$  is given in Algorithm 1. Algorithm 2 is a subroutine for processing one time step.

## B. Quantum-circuit Monte Carlo algorithm

Using the Monte Carlo summation to compute the path-integral formula in Eq. (5), we need to choose two parameters  $N_s$  and  $M_s$ , which are the number of  $s$  samples and the number of shots per quantum circuit for evaluating  $\langle \psi_f | O_s | \psi_i \rangle$ , respectively. Because the transition amplitude is a complex number in general, the quantum computing returns two real numbers  $a_{R,s}$  and  $a_{I,s}$ , which are estimates of real and imaginary parts of  $e^{i\theta_s} \langle \psi_f | O_s | \psi_i \rangle$ , respectively. By computing expected values of  $a_{R,s}$  and  $a_{I,s}$ , we obtain the transition amplitude  $\langle \psi_f | e^{iHt} O e^{-iHt} | \psi_i \rangle$  up to the factor  $C_A^{2N}$ . QCMC is summarised in Algorithm 3.

---

### Algorithm 3 Quantum-circuit Monte Carlo.

---

```

1: Input  $F, h, \sigma, N, \Delta t, N_s, M_s$ .
2: for  $v = 1$  to  $N_s$  do  $\triangleright v$  is the label of  $s$  samples.
3:    $(W, \theta) \leftarrow \text{SAMGEN}(F, h, \sigma, N, \Delta t)$ 
4:    $(a_{R,v}, a_{I,v}) \leftarrow \text{QUANTUMCIRCUITS}(\dots, W, \theta, M_s)$ 
5:    $\hat{A} \leftarrow C_A^{2N} \frac{1}{N_s} \sum_{v=1}^{N_s} (a_{R,v} + ia_{I,v})$ 
6: Output  $\hat{A}$  as the estimate of  $\langle \psi_f | e^{iHt} O e^{-iHt} | \psi_i \rangle$ .

```

---

## C. Quantum-circuit Monte Carlo on classical computer

In this section, we show that QCMC with the zeroth-order POE formula is equivalent to QMC on a classical computer. In the zeroth-order POE formula, the time evolution operator is expanded into the form  $e^{-iH\Delta t} = \sum_s c(s) \sigma_s$ , where  $\sigma_s \in \mathcal{P}_n$  are Pauli operators. We can express a Pauli operator as

$$\sigma = i^{x_1 z_1} X^{x_1} Z^{z_1} \otimes \dots \otimes i^{x_n z_n} X^{x_n} Z^{z_n}, \quad (44)$$

where  $x_a, z_a = 0, 1$ , and  $i^{x_a z_a} X^{x_a} Z^{z_a} = I, X, Y, Z$  is a single-qubit Pauli operator of the qubit- $a$ . We consider computational basis states in the form  $\bigotimes_{a=1}^n |\mu_a\rangle$ , where  $\mu_a = 0, 1$ . A Pauli operator acting on a basis state always results in a basis state, i.e.  $\sigma \bigotimes_{a=1}^n |\mu_a\rangle = \bigotimes_{a=1}^n i^{x_a z_a} (-1)^{z_a \mu_a} |\mu_a \oplus x_a\rangle$ , where  $\oplus$  denotes the modulo 2 addition. Therefore, Pauli operators acting on basis states can be efficiently calculated on a classical computer. Similarly, Pauli operators acting on product states in the form  $\bigotimes_{j=1}^n |\psi_j\rangle$  and stabiliser states  $|\rangle$  can also be efficiently calculated on a classical computer. In the following, we focus on computational basis states.

The zeroth-order POE formula is auxiliary-field Monte Carlo that takes the space of Pauli operators as the auxiliary-field. Suppose that the initial and final states are computational basis states and  $O$  is a Pauli operator, we can evaluate

$$\langle \psi_f | O_s | \psi_i \rangle = \langle \psi_f | \sigma_{s'_1} \cdots \sigma_{s'_N} O \sigma_{s_N} \cdots \sigma_{s_1} | \psi_i \rangle \quad (45)$$

on a classical computer. By expressing initial and final states as linear combinations of basis states and the operator  $O$  as a linear combination of Pauli operators, we can

evaluate  $\langle \psi_f | O_s | \psi_i \rangle$  on a classical computer for the general states and operator. Therefore, we can implement QCMC with the zeroth-order POE formula without using a quantum computer.

Now, we consider a class of Hamiltonians without short-time interference between Pauli operators. Each Pauli operator corresponds to two binary strings  $(x_1, \dots, x_n)$  and  $(z_1, \dots, z_n)$ . If the  $x$  strings of two Pauli operators  $\sigma$  and  $\tau$  are different, we have  $\langle \psi | \tau \sigma | \psi \rangle = 0$  for all computational basis states  $|\psi\rangle = \bigotimes_{a=1}^n |\mu_a\rangle$ . The short-time evolution operator  $e^{-iH\Delta t} \simeq \mathbb{1} - iH\Delta t$  acting on a basis state results in

$$e^{-iH\Delta t} |\psi\rangle \simeq |\psi\rangle - i\Delta t \sum_j h_j \sigma_j |\psi\rangle. \quad (46)$$

We can find that there is not any interference between the terms if and only if  $\langle \psi | \tau \sigma | \psi \rangle = 0$  for all  $\sigma, \tau \in \{\mathbb{1}\} \cup \{\sigma_i\}$ : i.e. Pauli operators in the Hamiltonian have different  $x$  strings.

For Hamiltonians without short-time interference, the zeroth-order POE formula is equivalent to Green's function Monte Carlo that takes the computational basis. In Green's function Monte Carlo, we sample states  $|\mathbf{r}\rangle$ ; In QCMC, we sample Pauli operators. Substituting the computational basis for  $\{|\mathbf{r}\rangle\}$ , the transition amplitude of each time step reads  $\langle \psi' | e^{-iH\Delta t} | \psi \rangle$ , where  $|\psi'\rangle = \bigotimes_{a=1}^n |\mu'_a\rangle$ . For a Hamiltonian without short-time interference, basis states  $|\psi'\rangle$  with nonzero  $\langle \psi' | e^{-iH\Delta t} | \psi \rangle$  and Pauli operators in  $\{\mathbb{1}\} \cup \{\sigma_i\}$  have one-to-one correspondence in the limit of small  $\Delta t$ . Therefore, sampling Pauli operators is equivalent to sampling basis states  $|\psi'\rangle$ .

The class of Hamiltonians without short-time interference includes those are hard for simulation in classical computing. In Appendix B, we show that the Fermi-Hubbard model on any bipartite lattice (e.g. the square lattice) can be encoded into a qubit Hamiltonian without short-time interference, using the Jordan-Wigner transformation.

## VI. QUANTUM CIRCUITS

We propose quantum circuits for evaluating the transition amplitude of the operator  $O_s$ , and the circuit depth is moderately increased upon the Lie-Trotter-Suzuki product. To measure the transition amplitude, we need to introduce an ancillary qubit, which controls the evolution of  $n$  qubits representing the system. In Eq. (42), the evolution is driven by Lie-Trotter-Suzuki products  $R_1$  and correction operators  $W$ . Our circuits are simplified in two ways: First, we avoid controlled Lie-Trotter-Suzuki products and only use controlled corrections; Second, correction operators are either Pauli operators  $\sigma$  or rotation operators  $e^{-i\phi\sigma}$ .

We propose two types of circuits. For compact circuits, the circuit depth is the same as the Lie-Trotter-Suzuki decomposition with additional controlled-correction gates.

For forward-backward circuits, the circuit depth is doubled, but they provide inherent quantum error mitigation. In this section, we also show how to efficiently decompose a controlled-correction gate into elementary gates. We assume that  $O$  is a unitary operator, and we can evaluate a general operator by decomposing it into a linear combination of unitary operators.

### A. Compact circuit

The compact circuit for second-order formulas is shown in Fig. 2(a). Circuits for other summation formulas are similar. For the first-order formulas, we remove  $S'_1$  products from the circuit; for the zeroth-order formulas, we remove both  $S_1$  and  $S'_1$  products; and by adding more  $S_1$  and  $S'_1$  products, the circuit can be used for higher-order formulas. If we ignore controlled-correction gates, the compact circuit for the  $l$ th-order summation formula is the same as the circuit for the  $l$ th-order Lie-Trotter-Suzuki product formula.

Now, we focus on second-order formulas, and the analysis for other formulas is similar. The final state of the compact circuit (before the basis adjusting gate  $B$ ) is

$$|\Psi\rangle = \frac{1}{\sqrt{2}} (|0\rangle_a \otimes OS'_1 W_N S_1 \cdots S'_1 W_1 S_1 |\psi_i\rangle + |1\rangle_a \otimes S'_1 W'_N S_1 \cdots S'_1 W'_1 S_1 |\psi_f\rangle). \quad (47)$$

Measuring the ancillary qubit, we get

$$\langle \Psi | X_a | \Psi \rangle = \text{Re} (\langle \psi_f | O_s | \psi_i \rangle), \quad (48a)$$

$$\langle \Psi | Y_a | \Psi \rangle = -\text{Im} (\langle \psi_f | O_s | \psi_i \rangle), \quad (48b)$$

where  $X_a$  and  $Y_a$  are Pauli operators of the ancillary qubit. Here, we have used Eq. (42). The procedure for evaluating  $\langle \psi_f | O_s | \psi_i \rangle$  using compact circuits is given in Algorithm 4.

---

#### Algorithm 4 Quantum circuit evaluation.

---

```

1: function QUANTUMCIRCUITS( $\mathbf{h}, \sigma, N, \Delta t, \mathbf{W}, \theta, M_s$ )
2:    $a_R, a_I \leftarrow 0$ 
3:   for  $i = 1$  to  $M_s$  do
4:     Implement the circuit, measure  $\cos \theta X_a + \sin \theta Y_a$ 
       and collect the outcome  $\mu_R = \pm 1$ .
5:      $a_R \leftarrow a_R + \mu_R$ 
6:     Implement the circuit, measure  $\sin \theta X_a - \cos \theta Y_a$ 
       and collect the outcome  $\mu_I = \pm 1$ .
7:      $a_I \leftarrow a_I + \mu_I$ 
8:    $a_R \leftarrow a_R / M_s$ 
9:    $a_I \leftarrow a_I / M_s$ 
10:  Output  $(a_R, a_I)$ .

```

---

### B. Forward-backward circuit

The forward-backward circuit for second-order formulas is shown in Fig. 2(b). Compared with the compact

circuit, the number of  $S_1$  and  $S'_1$  products is doubled. The final state of the circuit is

$$|\Phi\rangle = \frac{1}{\sqrt{2}} \left( |0\rangle_a \otimes |0\rangle^{\otimes n} + |1\rangle_a \otimes U_f^\dagger O_s |\psi_i\rangle \right). \quad (49)$$

Here, we have used Eq. (42). Measuring the ancillary qubit, we get

$$\langle \Phi | X_a | \Phi \rangle = \text{Re} (\langle \psi_f | O_s | \psi_i \rangle), \quad (50a)$$

$$\langle \Phi | Y_a | \Phi \rangle = \text{Im} (\langle \psi_f | O_s | \psi_i \rangle). \quad (50b)$$

The procedure for evaluating  $\langle \psi_f | O_s | \psi_i \rangle$  is similar to Algorithm 4. Note that evaluating the transition amplitude in this way does not provide inherent error mitigation. We discuss the inherent error mitigation using postselection in Sec. VIII B.

### C. Controlled-correction gates

We consider two types of qubit networks. On the all-to-all network, controlled-NOT gates on all pairs of qubits are available. On the linear network, only controlled-NOT gates on nearest neighboring qubits are allowed. We use  $\Lambda_{a,b}$  to denote the controlled-NOT gate that  $a$  and  $b$  are the control and target qubits, respectively. Because the error rate of controlled-NOT gates is usually much higher than single-qubit gates, we only count controlled-NOT gates and minimise their number.

A general Pauli operator  $\sigma$  is equivalent to an  $X$ -product Pauli operator (i.e. a tensor product of  $I$  and  $X$ ) up to a unitary transformation. For the  $\sigma$  in Eq. (44), the transformation is  $\tilde{R} = H^{z_1(1-x_1)} S^{z_1 x_1} \otimes \cdots \otimes H^{z_n(1-x_n)} S^{z_n x_n}$ , where  $H$  is the Hadamard gate, and  $S$  is the  $\frac{\pi}{4}$  phase gate. This transformation leads to  $\tilde{\sigma} = \tilde{R}^\dagger \sigma \tilde{R} = X^{x_1 \vee z_1} \otimes \cdots \otimes X^{x_n \vee z_n}$ , where  $x_a \vee z_a = 1 - (1 - x_a)(1 - z_a)$ .

Implementing the controlled- $\tilde{\sigma}$  gate on the all-to-all network is straightforward: For each qubit with  $x_a \vee z_a = 1$ , we apply the controlled-NOT gate  $\Lambda_{0,a}$ , where qubit-0 is the ancillary qubit. The controlled- $\tilde{\sigma}$  gate is  $\prod_{a=1}^n \Lambda_{0,a}^{x_a \vee z_a}$ , and the number of controlled-NOT gates is  $N_\Lambda = \sum_{a=1}^n x_a \vee z_a \leq n$ .

In the compact circuit shown in Fig. 2(a), there are two controlled-correction gates in each time step, corresponding to  $W_i$  and  $W'_i$ , respectively. When  $W_i = \tau$  and  $W'_i = \tau'$  are Pauli operators, we can combine the two controlled-correction gates into one controlled- $\sigma$  gate in the following way. Note that  $\tau' \tau = \zeta \sigma$ , where  $\zeta$  is a phase factor. We apply  $\tau$  first, then a controlled- $\sigma$  gate, and finally a phase gate  $\text{diag}(1, \zeta)$  on the ancillary qubit. The overall transformation is equivalent to the two controlled-correction gates. The total number of controlled-NOT gates is  $N_\Lambda$ .

Now, we present another protocol for the controlled- $\sigma$  gate. The circuit is shown in Fig. 3(a), which is formed of three parts: gates transforming a general Pauli operator

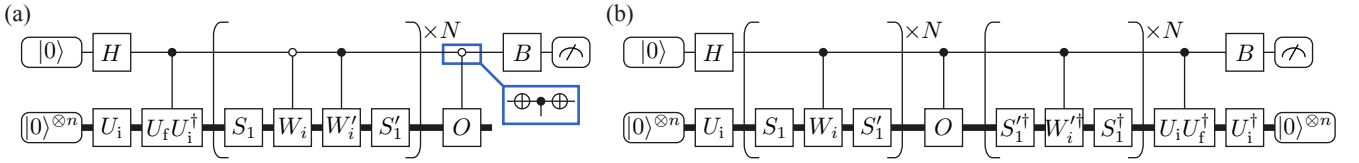


FIG. 2. Quantum circuits for evaluating  $e^{i\theta_s} \langle \psi_f | O_s | \psi_i \rangle$ . The qubit on the top is the ancillary qubit. The empty circle in the blue box denotes a controlled- $U$  gate that  $U$  acts on the  $n$  qubits when the ancillary qubit is in  $|0\rangle$ . Unitary operators  $U_i$  and  $U_f$  prepare the initial and final states, respectively, i.e.  $|\psi_i\rangle = U_i|0\rangle^{\otimes n}$  and  $|\psi_f\rangle = U_f|0\rangle^{\otimes n}$ . The gate  $B$  is for adjusting the measurement basis. For simplicity, we use notations  $S_1 = S_1(\frac{\Delta t}{2})$  and  $S'_1 = S_1(-\frac{\Delta t}{2})^\dagger$ .

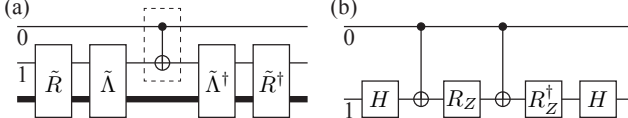


FIG. 3. (a) Circuit of the controlled- $\sigma$  gate. Qubit-0 is the ancillary qubit. (b) Circuit of the controlled- $e^{-i\phi X_1}$  gate. Replacing the controlled-NOT gate in the dashed box with the controlled- $e^{-i\phi X_1}$  gate, we have the circuit of controlled- $e^{-i\phi\sigma}$  gate. The single-qubit phase gate  $R_Z = e^{i\frac{\phi}{2}Z}$ .

$\sigma$  into an  $X$ -product Pauli operator  $\tilde{\sigma}$ , gates transforming  $\tilde{\sigma}$  into the single-qubit Pauli operator  $X_1$  on qubit-1, and the controlled-NOT gate  $\Lambda_{0,1}$  on the ancillary qubit and qubit-1. On the linear network, we assume that qubit-1 is next to the ancillary qubit. On the all-to-all network, we can label any qubit as qubit-1; without loss of generality, we assume  $x_1 \vee z_1 = 1$ . In this protocol, there is only one instead of  $N_\Lambda$  gates on the ancillary qubit. Because the outcome is obtained by measuring the ancillary qubit, applying less gates on the ancillary qubit potentially reduces the impact of errors. Replacing  $\Lambda_{0,1}$  with the circuit in Fig. 3(b), we can realise the controlled- $e^{-i\phi\sigma}$  gate.

To transform  $\tilde{\sigma}$  into  $X_1$ , we look for a transformation  $\tilde{\Lambda}$  that satisfies  $\sigma = \tilde{\Lambda}^\dagger X_1 \tilde{\Lambda}$ . On the all-to-all network, we take  $\tilde{\Lambda} = \prod_{a=2}^n \Lambda_{1,a}^{x_a \vee z_a}$ , and the number of controlled-NOT gates for each  $\tilde{\Lambda}$  is  $N_\Lambda - 1$ . On the linear network, we take

$$\tilde{\Lambda} = \Lambda_{1,2} \Lambda_{2,1}^{x_1 \downarrow z_1} \Lambda_{2,3} \Lambda_{3,2}^{x_2 \downarrow z_2} \cdots \Lambda_{n'-1,n'} \Lambda_{n',n'-1}^{x_{n'-1} \downarrow z_{n'-1}}, \quad (51)$$

where  $x_a \downarrow z_a = (1 - x_a)(1 - z_a)$  and  $n' = \max\{a \mid x_a = 1\}$ . On the linear network, the number of controlled-NOT gates for each  $\tilde{\Lambda}$  is  $(n' - 1) + \sum_{a=1}^{n'-1} x_a \downarrow z_a \leq 2n - 2$ .

The maximum number of controlled-NOT gates for implementing the two controlled-correction gates in each time step is summarised as follows. On the all-to-all network, the maximum gate number is  $n$  for POE formulas, which becomes  $2(n - 1) + 1 = 2n - 1$  to reduce gates on the ancillary qubit, and  $2[2(n - 1) + 2] = 4n$  for LOR formulas. On the linear network, the maximum gate number is  $2(2n - 2) + 1 = 4n - 3$  for POE formulas.

las and  $2[2(2n - 2) + 2] = 8n - 4$  for LOR formulas. In the MCQC algorithm, controlled-correction gates are randomly selected, and the gate number could be much smaller than its maximum value. For example, for the POE formula, usually the Pauli operator is identity with the highest probability.

## VII. OPTIMAL DISTRIBUTION

In this section, we derive the optimal distribution of  $\mathbf{s}$  that minimises the variance in Monte Carlo. Using protocols in Sec. VI to evaluate  $\langle \psi_f | O_s | \psi_i \rangle$ , we prove that taking the distribution in Eq. (7) and  $M_s = 1$  is optimal, and the minimum variance is given by Eq. (13).

A quantum circuit usually has random measurement outcomes, therefore, outputs of quantum computing  $a_{R,s}$  and  $a_{I,s}$  are random variables. We suppose that  $a_{\nu,s}$  ( $\nu = R, I$ ) takes the value  $a_i$  with the probability  $P_{\nu,s,i}$  in the quantum computing, then its expected value is  $E[a_{\nu,s}]_{qc} = \sum_i P_{\nu,s,i} a_i$ . Here,  $E[\bullet]_{qc}$  denotes the mean taken over quantum computing runs for the specific  $\mathbf{s}$  (each run returns an output evaluated using  $M_s$  shots), and  $E[\bullet]$  without the subscript ‘qc’ denotes the mean taken over both  $\mathbf{s}$  and quantum computing runs. Using protocols in Sec. VI,  $a_{R,s}$  and  $a_{I,s}$  are unbiased estimators of  $\langle \psi_f | O_s | \psi_i \rangle$ , i.e.

$$e^{i\theta_s} \langle \psi_f | O_s | \psi_i \rangle = E[a_{R,s}]_{qc} + i E[a_{I,s}]_{qc}. \quad (52)$$

Let  $A_R$  and  $A_I$  be the real and imaginary parts of  $\langle \psi_f | e^{iHt} O e^{-iHt} | \psi_i \rangle$ , respectively. In the QCMC algorithm, we evaluate the summation  $A_\nu = \sum_s c_s E[a_{\nu,s}]_{qc}$  using the Monte Carlo method, where  $c_s = \left| \prod_{i=1}^N c(s_i) c(s'_i)^* \right|$ . Given any probability distribution  $P(\mathbf{s})$ , we have

$$A_\nu = \sum_s P(\mathbf{s}) \frac{c_s E[a_{\nu,s}]_{qc}}{P(\mathbf{s})} = E \left[ \frac{c_s a_{\nu,s}}{P(\mathbf{s})} \right]. \quad (53)$$

Therefore, we can estimate  $A_\nu$  by sampling  $\mathbf{s}$  according to the distribution  $P(\mathbf{s})$  and compute the empirical mean of  $c_s a_{\nu,s} / P(\mathbf{s})$ . The variance of the estimator  $\hat{A}_\nu$  with

$N_s$  samples is

$$\begin{aligned}\text{Var}(\hat{A}_\nu) &= \frac{1}{N_s} \text{Var}\left(\frac{c_s a_{\nu,s}}{P(\mathbf{s})}\right) \\ &= \frac{1}{N_s} \sum_s \frac{c_s^2 \alpha_{\nu,s}^2}{P(\mathbf{s})} - \frac{A_\nu^2}{N_s},\end{aligned}\quad (54)$$

where  $\alpha_{\nu,s} = \sqrt{\text{E}[a_{\nu,s}^2]_{\text{qc}}}$ . The optimal distribution that minimises the variance is  $P(\mathbf{s}) \propto |c_s| \alpha_{\nu,s}$ , and the minimum variance is

$$\text{Var}(\hat{A}_\nu) = \frac{1}{N_s} \left( \sum_s |c_s| \alpha_{\nu,s} \right)^2 - \frac{A_\nu^2}{N_s}. \quad (55)$$

Now, we consider that  $a_{\nu,s}$  is obtained by taking the empirical mean of  $M_s$  binary numbers. Each binary number takes  $\pm 1$  corresponding to the measurement outcome of the ancillary qubit (see Algorithm 4). Then,  $a_{\nu,s}$  follows the binomial distribution, and

$$\alpha_{\nu,s} = \sqrt{\frac{1 + (M_s - 1)\text{E}[a_{\nu,s}]_{\text{qc}}^2}{M_s}}. \quad (56)$$

Let  $M_{\text{tot}}$  be the total number of circuit shots, we have  $N_s = M_{\text{tot}}/M_s$ . Substituting  $\alpha_{\nu,s}$  and  $N_s$  into Eq. (55), we obtain the variance as a function of  $M_s$ . Taking  $M_s$  as a continuous variable, we can find that the derivative of the variance with respect to  $M_s$  is always positive when  $M_s \geq 1$ . Therefore, the variance is minimised at  $M_s = 1$ . When  $M_s = 1$ , we have  $\alpha_{\nu,s} = 1$ , and the optimal distribution is  $P(\mathbf{s}) \propto |c_s|$ . Accordingly, the minimum variance is

$$\text{Var}(\hat{A}_\nu) = \frac{1}{M_{\text{tot}}} \left( \sum_s |c_s| \right)^2 - \frac{A_\nu^2}{M_{\text{tot}}}. \quad (57)$$

With  $\text{Var}(\hat{A}) = \text{Var}(\hat{A}_R) + \text{Var}(\hat{A}_I)$ , we obtain the minimum total variance in Eq. (13). Here, we have assumed that the total number of shots for each of the real and imaginary parts is  $M_{\text{tot}}$ .

We remark that the optimal distribution is obtained by assuming the empirical mean estimator for  $a_{\nu,s}$ . If we have the prior knowledge of  $a_{\nu,s}$  distribution, we can use other estimators such as the Bayes estimator to reduce the variance. In the extreme case, suppose that  $\text{E}[a_{\nu,s}]_{\text{qc}}$  is known, the optimal distribution is  $P(\mathbf{s}) \propto |c_s| \text{E}[a_{\nu,s}]_{\text{qc}}$  instead of  $P(\mathbf{s}) \propto |c_s| \alpha_{\nu,s}$  (Note that in this case we do not even need the quantum computer).

### VIII. QUANTUM ERROR MITIGATION

Many quantum error mitigation protocols can be classified into three categories. In the first category, with the knowledge of the error model, we compensate the effect of errors by using approaches such as error extrapolation and probabilistic error cancellation (i.e. quasi-probability decomposition) [65, 74, 76]. In the second

category, data from quantum circuits are processed according to constraints on the quantum state. Protocols in this category includes, for example, symmetry-based postselection [80, 81] and purification [82–84]. There are also protocols, e.g. subspace expansion [75], introduced for specific algorithms, which belong to the third category.

In this section, we first discuss the application of quasi-probability decomposition in QCMC, and then we show that the forward-backward circuit in Fig. 2(b) provides inherent error mitigation based on constraints on the state. The error mitigation increases the variance in Monte Carlo. On a noisy quantum computer, we need to choose an optimal time step size  $\Delta t$  to minimise the variance. Eventually, the variance is determined by the error rate, which is discussed in Sec. IX.

#### A. Quasi-probability decomposition

In the quasi-probability decomposition, an error-free quantum operation is expressed as a linear combination of noisy operations. Let  $\mathcal{G}^{\text{ef}} = [U]$  and  $\mathcal{G}_i$  be the error-free operation and noisy operations, respectively, the quasi-probability decomposition is in the form

$$\mathcal{G}^{\text{ef}} = \sum_i q_i \mathcal{G}_i, \quad (58)$$

where  $q_i$  are real coefficients, i.e. quasi-probabilities. Here,  $U$  is a unitary quantum gate,  $[U](\bullet) = U \bullet U^\dagger$  is the trace-preserving completely positive map of the gate, and  $\mathcal{G}_i$  are operations that can be actually implemented on the noisy quantum computer. Similar decompositions can be applied to the initial state and observable to be measured.

We take the Pauli error model as an example. Note that a general error model can be converted into the Pauli error model using Pauli twirling [85, 86]. In the Pauli error model, the noisy operation of a two-qubit gate  $U$  reads  $\mathcal{G} = \mathcal{N}[U]$ , where the noise map

$$\mathcal{N} = (1 - p)[I \otimes I] + \sum_{\sigma \in \{I, X, Y, Z\}^{\otimes 2} \setminus \{I \otimes I\}} p_\sigma [\sigma], \quad (59)$$

$p_\sigma \ll 1$  is the rate of Pauli error  $\sigma$ , and  $p = \sum_{\sigma \neq I \otimes I} p_\sigma$  is the total error rate. The inverse map of  $\mathcal{N}$  is also in the Pauli-operation summation form, i.e.

$$\mathcal{N}^{-1} = \sum_{\sigma \in \{I, X, Y, Z\}^{\otimes 2}} q_\sigma [\sigma], \quad (60)$$

and we can solve coefficients  $q_\sigma$  numerically. Without a general analytically expression of  $q_\sigma$ , it is sufficient for us to consider the first-order expansion in order to discuss the impact on variance. To the first order, we have

$$q_{I \otimes I} = 1 + p + O(p^2), \quad (61)$$

$$q_{\sigma \neq I \otimes I} = -p_\sigma + O(p^2). \quad (62)$$

Given the inverse map, the quasi-probability decomposition of gate  $U$  is

$$\mathcal{G}^{\text{ef}} = \sum_{\sigma \in \{I, X, Y, Z\}^{\otimes 2}} q_{\sigma} [\sigma] \mathcal{G}. \quad (63)$$

Assuming errors in single-qubit gates are negligible, the composite operation  $[\sigma] \mathcal{G}$  can be implemented on the noisy quantum computer by adding a Pauli gate  $\sigma$  after the noisy two-qubit gate  $\mathcal{G}$ . We note that the assumption of negligible errors in single-qubit gates is not necessary for the quasi-probability decomposition.

Now, we apply the quasi-probability decomposition to a quantum circuit. In QCMC using protocols in Sec. VI, only the ancillary qubit is measured. We can adjust the measurement basis using the gate  $B$  in Fig. 2, therefore, without loss of generality we focus on the observable  $Z_a$  in the error mitigation. Given a quantum circuit formed of many elementary gates, the mean of  $Z_a$  reads

$$\langle Z_a \rangle = \text{Tr} [Z_a \mathcal{G}_{N_G} \cdots \mathcal{G}_1(\rho)], \quad (64)$$

where  $\rho = |0\rangle\langle 0|^{\otimes n}$  is the initial state of quantum circuit, and  $N_G$  is the number of gates. Suppose the quasi-probability decomposition of each gate is  $\mathcal{G}_j^{\text{ef}} = \sum_i q_{j,i} \mathcal{G}_{j,i}$ , the error-free mean is

$$\begin{aligned} \langle Z_a \rangle^{\text{ef}} &= \sum_{i_1, \dots, i_{N_G}} \left( \prod_{j=1}^{N_G} q_{j,i} \right) \\ &\quad \times \text{Tr} [Z_a \mathcal{G}_{N_G, i_{N_G}} \cdots \mathcal{G}_{1, i_1}(\rho)]. \end{aligned} \quad (65)$$

The second line in the above equation is the mean of  $Z_a$  in a circuit modified from the original one. We remark that errors in the initial state and final measurement can be corrected in a similar way.

We evaluate the decomposition formula in Eq. (65) using the Monte Carlo summation method by sampling random noisy circuits, therefore, such an error mitigation protocol is called probabilistic error cancellation. Similar to QCMC, sampling random circuits increases the variance by a factor  $C_E^2$ , where  $C_E = \prod_{j=1}^{N_G} (\sum_i |q_{j,i}|)$ . According to the Pauli error model, we have  $C_E = \prod_{j=1}^{N_G} [1 + 2p_j + O(p_j^2)]$ , where  $p_j$  is the error rate of the  $j$ th gate. We can find that the factor  $C_E$  increases with the number of noisy gates. Therefore, the circuit with less gates, i.e. the compact circuit in Fig. 2(a), is preferred.

In previous discussions, we have assumed that errors in different gates are not correlated. To deal with correlations, we need to introduce a general form of the quasi-probability decomposition,

$$\langle Z_a \rangle_{\mathbf{C}_0}^{\text{ef}} = \sum_k q_k \langle Z_a \rangle_{\mathbf{C}_k}, \quad (66)$$

where  $\langle Z_a \rangle_{\mathbf{C}_k}$  is the mean of  $Z_a$  in the circuit  $\mathbf{C}_k$ ,  $\mathbf{C}_0$  is the original circuit, and  $\mathbf{C}_{k \neq 0}$  are modified circuits. Modified circuits generated by adding single-qubit operations to the original circuit are usually sufficient for the

existence of the decomposition formula. Without correlations, we can work out quasi-probabilities using gate set tomography [76]; with correlations, we can determine quasi-probabilities using data of Clifford circuits, i.e. Clifford sampling [87, 88]. Given the quasi-probability decomposition formulas, we can evaluate  $\langle \psi_f | O_s | \psi_i \rangle$  with error mitigation following the procedure in Algorithm 5.

---

**Algorithm 5** Quantum circuit evaluation with error mitigation.

---

Input  $\mathbf{h}, \sigma, N, \Delta t, \mathbf{W}, \theta, M_s, \nu$ .

- 1: Compose the circuit  $\mathbf{C}_0$  according to input parameters, in which  $\nu = R, I$  (real or imaginary) determines the basis adjusting gate  $B$  in Fig. 2.
- 2: Work out the decomposition formula in Eq. (66).
- 3:  $C_E \leftarrow \sum_k |q_k|$
- 4:  $a_{\nu} \leftarrow 0$
- 5: **for**  $i = 1$  to  $M_s$  **do**
- 6:     Choose  $k$  with the probability  $|q_k|/C_E$ .
- 7:     Implement the circuit  $\mathbf{C}_k$ , measure  $Z_a$  and collect the outcome  $\mu = \pm 1$ .
- 8:      $a_{\nu} \leftarrow a_{\nu} + C_E \mu$
- 9:  $a_{\nu} \leftarrow a_{\nu}/M_s$
- 10: Output  $a_{\nu}$ .

---

## B. Inherent error mitigation by postselection

As shown in verified quantum phase estimation [89] and dual-state purification [90], a quantum circuit with the forward-backward structure incorporating the postselection is robust to errors. For the postselection, we measure the  $n$  qubits representing the system in addition to the ancillary qubit, see Fig. 2(b). We only select the state when the measurement outcome is  $|0\rangle^{\otimes n}$ , which transforms the final state in Eq. (49) into

$$|\Phi'\rangle = \frac{|0\rangle_a + \langle \psi_f | O_s | \psi_i \rangle |1\rangle_a}{\sqrt{1 + |\langle \psi_f | O_s | \psi_i \rangle|^2}} \otimes |0\rangle^{\otimes n}. \quad (67)$$

Measuring the ancillary qubit in the state after postselection, we have

$$\langle X_a \rangle_0 = \frac{2\text{Re}(\langle \psi_f | O_s | \psi_i \rangle)}{1 + |\langle \psi_f | O_s | \psi_i \rangle|^2}, \quad (68a)$$

$$\langle Y_a \rangle_0 = \frac{2\text{Im}(\langle \psi_f | O_s | \psi_i \rangle)}{1 + |\langle \psi_f | O_s | \psi_i \rangle|^2}, \quad (68b)$$

$$\langle Z_a \rangle_0 = \frac{1 - |\langle \psi_f | O_s | \psi_i \rangle|^2}{1 + |\langle \psi_f | O_s | \psi_i \rangle|^2}, \quad (68c)$$

where  $\langle \bullet \rangle_0$  denotes the mean conditioned on the outcome  $|0\rangle^{\otimes n}$ . Solving the equations, we get

$$\langle \psi_f | O_s | \psi_i \rangle = \frac{\langle X_a \rangle_0 + i \langle Y_a \rangle_0}{1 + \langle Z_a \rangle_0}. \quad (69)$$

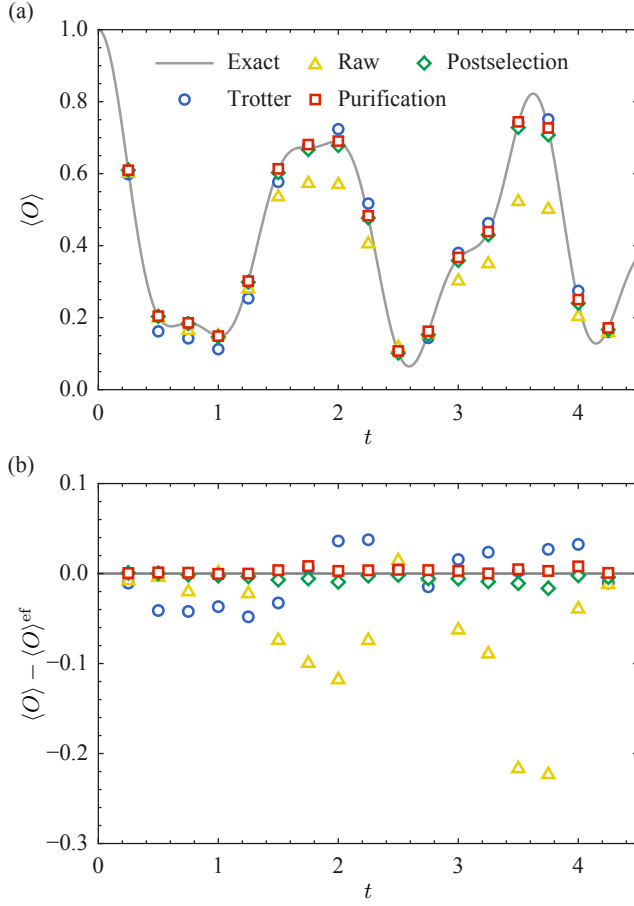


FIG. 4. (a) Observable  $\langle O \rangle$  as a function of the time  $t$ . In the simulation, we take  $J = U = 1$  and  $\Delta t = 0.05$ . The raw data is obtained using the forward-backward circuit without error mitigation, according to Eq. (50). With the postselection, the observable is computed according to Eq. (69). The tomography purification is used to further reduce the error. As a comparison, the Lie-Trotter-Suzuki product formula is evaluated without machine errors. (b) Error  $\langle O \rangle - \langle O \rangle^{\text{ef}}$  in the observable. Here,  $\langle O \rangle^{\text{ef}}$  denotes the exact value.

The postselection forces most of qubits into a pure state, which eliminates errors that transform  $|0\rangle^{\otimes n}$  into orthogonal states. In addition to the postselection, we can purify the ancillary qubit as follows. According to Eq. (67), the state of the ancillary qubit is a pure state when the quantum circuit is error-free. In the tomography purification, we implement the state tomography to the ancillary qubit and compute the eigenstate with the largest eigenvalue of the reconstructed reduced density matrix [90]. Using the eigenstate to compute the three means  $\langle \bullet \rangle_0$ , we can make sure that the final result is obtained from a pure state. In Sec. VII B 1, we demonstrate that the inherent error mitigation can significantly reduce the error in QCMC.

Now, we have two protocols using the circuit in Fig. 2(b) to evaluate  $\langle \psi_f | O_s | \psi_i \rangle$ . In the protocol without

postselection (see Sec. VII B), the estimator of  $\langle \psi_f | O_s | \psi_i \rangle$  is unbiased, and it is optimal to take  $M_s = 1$ . In the protocol with postselection, the estimator is biased due to the denominator in Eq. (69), i.e. the mean of estimates is not exactly  $\langle \psi_f | O_s | \psi_i \rangle$  when  $M_s$  is finite. Therefore, for the postselection protocol, it is necessary to choose a large  $M_s$  to evaluate each  $\langle \bullet \rangle_0$  (such that the bias is small) in order to obtain an accurate final result of the transition amplitude.

The inherent error mitigation increases the variance of QCMC. When the circuit is error-free, the postselection succeeds with the probability

$$P_S = \frac{1}{2} \left( 1 + |\langle \psi_f | O_s | \psi_i \rangle|^2 \right) \geq \frac{1}{2}. \quad (70)$$

If the circuit is implemented for  $M_s$  shots, only  $P_S M_s$  shots generate effective data on average. When the circuit is noisy, errors transform  $|0\rangle^{\otimes n}$  into orthogonal states, which reduces the success rate. Therefore, the number of effective shots decreases with the error rate and the gate number, which causes an enlarged variance.

### 1. Numerical demonstration

To demonstrate the inherent error mitigation, we consider the one-dimensional Fermi-Hubbard model and numerically simulate the noisy quantum computing on a classical computer. The Hamiltonian reads

$$H = -J \sum_{i=1}^{N_L-1} \sum_{s=\uparrow,\downarrow} \left( c_{i,s}^\dagger c_{i+1,s} + c_{i+1,s}^\dagger c_{i,s} \right) + U \sum_i c_{i,\uparrow}^\dagger c_{i,\uparrow} c_{i,\downarrow}^\dagger c_{i,\downarrow}, \quad (71)$$

where  $N_L = 3$  is the number of sites, and  $c_{i,s}$  is the annihilation operator for the fermion with spin- $s$  on the  $i$ th site. This model can be encoded into  $2N_L$  qubits using the Jordan-Wigner transformation.

We use the first-order Lie-Trotter-Suzuki product formula and a corresponding summation formula to simulate the real time evolution. The initial state is  $|\psi_i\rangle = c_{1,\uparrow}^\dagger c_{2,\downarrow}^\dagger c_{3,\uparrow}^\dagger |\text{Vac}\rangle$ , where  $|\text{Vac}\rangle$  is the vacuum state, and we take  $|\psi_f\rangle = |\psi_i\rangle$ . The observable is  $O = 2c_{3,\uparrow}^\dagger c_{3,\uparrow} - \mathbb{1}$ , and the simulation is to compute  $\langle O \rangle = \langle \psi_i | e^{iHt} O e^{-iHt} | \psi_i \rangle$ . To minimise the variance of QCMC, we first expand the correction operator using Pauli operators, i.e.

$$V_1 = \sum_{\sigma \in \mathcal{P}_n} (a_\sigma - i b_\sigma) \sigma, \quad (72)$$

where  $a_\sigma$  and  $b_\sigma$  are real, and

$$a_\sigma - i b_\sigma = 2^{-n} \text{Tr} [\sigma e^{-iH\Delta t} S_1 (\Delta t)^\dagger]. \quad (73)$$

We have  $a_{\mathbb{1}} > 0$  and  $b_{\mathbb{1}} = 0$ . Then, we take the summation formula

$$e^{-iH\Delta t} = \sum_{\sigma \in \mathcal{P}_n \setminus \{\mathbb{1}\}} (a_\sigma \sigma + \beta_\sigma e^{-i\text{sgn}(b_\sigma) \phi} \sigma) S_1, \quad (74)$$

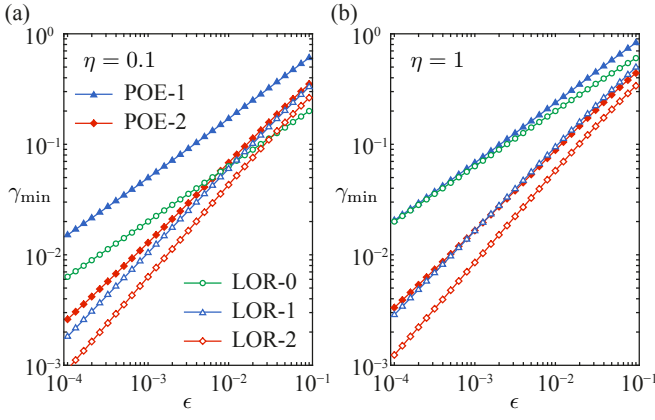


FIG. 5. The minimum variance increasing rate  $\gamma_{\min}$ .  $\epsilon$  is the error rate of one elementary Lie-Trotter-Suzuki product  $S_1$ .  $\eta\epsilon$  is the average error rate of controlled-correction gates in one time step. POE- $l$  denotes  $l$ th-order POE formula, and LOR- $l$  denotes  $l$ th-order LOR formula.

where  $\phi = \arctan(a_{\perp}^{-1} \sum_{\sigma} |b_{\sigma}|)$  and  $\beta_{\sigma} = |b_{\sigma}| / \sin \phi$ .

Using the forward-backward circuit for error mitigation, we find that the impact of machine errors can be significantly suppressed, as shown in Fig. 4. We model the noise in quantum computing using the depolarising error model. For a controlled-NOT gate, the noise map is given by Eq. (59) with parameters  $p_{\sigma} = p/15$ . We neglect errors in the initialisation, single-qubit gates and measurement. In the numerical simulation, we take the error rate per gate  $p = 0.03\%$ . The number of controlled-NOT gates for each  $S_1$  is 14, and the simulation involves at most 85 time steps, i.e. the total number of controlled-NOT gates is above 2380. Therefore, the maximum total error rate is above 71.4%. After the error mitigation, we find that the overall accuracy of the summation formula taking  $N_s = 10000$  samples is higher than the product formula without machine errors.

## IX. QUANTUM COMPUTING VERSUS CLASSICAL COMPUTING

Sampling noise limits the accuracy of the QCMC algorithm. The variance of QMC increases exponentially with the evolution time as  $\sim \frac{1}{N_s} C_A^{4N} = \frac{1}{N_s} e^{4t\Delta t^{-1} \ln C_A}$ . As summarised in Table I,  $C_A = 1 + \xi \Delta t^k + O(\Delta t^{k+1})$ , where  $\xi$  is a constant depending on the Hamiltonian. When  $k > 1$ , by taking  $\Delta t = \left(\frac{\delta}{4t\xi}\right)^{1/(k-1)}$ , we can reduce the factor to  $C_A^{4N} = e^{\delta+O(\delta^{k/(k-1)})}$  for any small  $\delta$ . We note that  $k > 1$  in  $l$ th-order POE formulas with  $l > 0$  and all LOR formulas. For the zeroth-order POE formula, because  $C_A = e^{h_{\text{tot}}\Delta t}$  (i.e.  $k = 1$ ), we have  $C_A^{4N} = e^{4h_{\text{tot}}t}$  for all  $\Delta t$ .

It is widely believed that a classical computer cannot simulate the time evolution of general quantum many-

body systems at a polynomial cost, which is one of main motivations for quantum computing [1]. The QCMC algorithm with the zeroth-order POE formula is equivalent to a classical algorithm, i.e. Green's function Monte Carlo taking the computational basis, for a large class of Hamiltonians (see Sec. V C). In this classical algorithm, the variance increases exponentially with the evolution time and system size, i.e.  $\sim \frac{1}{N_s} e^{4h_{\text{tot}}t}$ , whatever  $\Delta t$  we choose. Here,  $t$  is the evolution time, and  $h_{\text{tot}}$  increases with the system size. The variance is up to minimization, e.g. changing the Hilbert space basis [27] and optimising the way of generating samples. Nevertheless, the existence of a generic approach that reduces the exponential scaling to polynomial one is unlikely [33].

On a fault-tolerant quantum computer, we can simulate the time evolution of quantum many-body systems at a polynomial cost. By taking a small  $\Delta t$ , we can reduce the factor  $C_A^{4N}$  to a satisfactory level, and  $\Delta t$  scales polynomially with  $t$  and  $h_{\text{tot}}$ . Therefore, the number of time steps  $N = t/\Delta t$ , i.e. the circuit depth, scales polynomially with  $t$  and  $h_{\text{tot}}$ .

On a noisy quantum computer, the cost of simulating quantum many-body systems increases exponentially with the evolution time and system size, and the increasing rate decreases with the error rate. Using the quasi-probability decomposition to mitigate errors, the error mitigation enlarges the variance. The variance taking into account quantum error mitigation is  $\sim \frac{1}{N_s} C_A^{4N} C_E^2$ . We consider the compact circuit in Fig. 2(a). Let  $\epsilon$  be the error rate of one elementary product  $S_1$  (we assume that  $S'_1$  has the same error rate),  $g$  be the number of  $S_1$  and  $S'_1$  products per time step and  $\eta\epsilon$  be the average error rate of controlled-correction gates in one time step, the total error rate of one time step is approximately  $(g + \eta)\epsilon$ . Here,  $g = 0, 1, 2$  for zeroth-, first- and second-order formulas, respectively. Suppose the total error rate of other operations [which are out of the bracket in Fig. 2(a)] is  $\epsilon'$ , the factor due to error mitigation is  $C_E \simeq (1 + 2\epsilon') [1 + 2(g + \eta)\epsilon]^N$ , according to the Pauli error model. Then, we can express the variance in the form

$$\frac{1}{N_s} C_A^{4N} C_E^2 \simeq \frac{1}{N_s} (1 + 2\epsilon')^2 e^{4\gamma h_{\text{tot}}t}, \quad (75)$$

where

$$\gamma = \frac{1}{h_{\text{tot}}\Delta t} \ln \left[ C_A \sqrt{1 + 2(g + \eta)\epsilon} \right]. \quad (76)$$

We can find that the rate  $\gamma$  decreases with the error rate.

Given the error rate of the noisy quantum computer, we choose the time step size  $\Delta t$  to minimise the rate  $\gamma$ . Taking  $C_A \simeq 1 + \xi \Delta t^k$ , we can find that the optimal step size is

$$\Delta t_{\text{opt}} \simeq \left[ \frac{(g + \eta)\epsilon}{(k-1)\xi} \right]^{1/k}, \quad (77)$$

and the corresponding minimum rate is

$$\gamma_{\min} \simeq \frac{k\xi^{1/k}}{h_{\text{tot}}} \left[ \frac{(g + \eta)\epsilon}{k-1} \right]^{\frac{k-1}{k}}. \quad (78)$$

For the second-order LOR formula,  $k = 6$ ,  $g = 2$  and  $\xi < h_{\text{tot}}^6/(2 \times 18^2)$ . In Fig. 5, we plot the minimum rate computed numerically using formulas of  $C_A$  in Table I. For the first- and second-order formulas, we take the upper bound of simplified leading-order contribution. We can find that the second-order LOR formula outperforms other formulas. Taking higher-order formulas does not further reduce  $\gamma$  for the given error rates.

Although the cost of the QCMC algorithm on a noisy quantum computer scales exponentially with the evolution time and system size as the same as the classical algorithm, the quantum computing can accelerate QMC by reducing the variance. To achieve the computation accuracy  $\delta$ , i.e. reduce the variance to  $\delta^2$ , we take  $N_s \sim e^{4\gamma h_{\text{tot}} t}/\delta^2$ . In the classical algorithm,  $\gamma = 1$ . In the quantum algorithm, taking the minimum value for  $\eta = 1$  [see Fig. 5(b)], we have  $\gamma \simeq 0.34$  when the error rate per elementary product is  $\epsilon = 0.1$  and  $\gamma \simeq 0.058$  when  $\epsilon = 0.01$ . For  $h_{\text{tot}} t = 4$ , the quantum algorithm reduces the sample size  $N_s$  by a factor of  $\sim 4 \times 10^4$  when  $\epsilon = 0.1$  and  $\sim 4 \times 10^6$  when  $\epsilon = 0.01$ . The advantage of quantum algorithm grows when the error rate decreases; fitting to the second-order LOR curve in Fig. 5(b), we have  $\gamma \simeq 2.45\epsilon^{0.82}$ .

We can reduce the variance by optimising the quantum algorithm. First, we can significantly reduce  $C_A$  for a Hamiltonian with only local interactions.  $C_A$  is greater than one because of the correction operator, which is used to compensate the difference between the exact time evolution operator and the Lie-Trotter-Suzuki product. According to the Baker-Campbell-Hausdorff formula, this difference is a series of commutators. For local interactions, most of the commutators in low-order terms are zero. In this case, expanding the correction operator according to the Baker-Campbell-Hausdorff formula (instead of the direct Taylor expansion) can reduce  $C_A$ . Second, similar to the classical algorithm, with the knowledge of  $\langle \psi_f | O_s | \psi_i \rangle$ , we can optimise the distribution of generating samples to reduce the variance. Thirdly, the

variance due to quantum error mitigation can be reduced. In the error mitigation protocol used to estimate  $\gamma$ , we correct all Pauli errors in the circuit, which is unnecessary. Because the ancillary qubit is measured to evaluate the transition amplitude, we only need to correct errors that affect the ancillary qubit. These errors can be identified and corrected by utilising the learning-based approach of error mitigation [87].

## X. CONCLUSIONS

In this paper, we propose a QMC algorithm that uses quantum computing as a subroutine. In our algorithm, we use exact summation formulas to express the time evolution operator. We optimise these formulas and quantum circuits to minimise the Monte Carlo variance and circuit depth. The optimal distribution of generating samples in Monte Carlo is derived in the circumstances of probabilistic evaluation using quantum computing. On a fault-tolerant quantum computer, the complexity of our algorithm is polynomial. On a noisy quantum computer with a finite error rate, we can use probabilistic error cancellation or inherent error mitigation to eliminate machine errors. Although the complexity is exponential on a noisy quantum computer, we find that the impact of sign problem can be substantially reduced in our algorithm. Our result shows that a near-term quantum computer without fault tolerance can speed up meaningful computing tasks, such as the non-variational simulation of quantum many-body systems.

## ACKNOWLEDGMENTS

We acknowledge the use of simulation toolkit QuESTlink [91] for this work. We acknowledge the support of the National Natural Science Foundation of China (Grant No. 11875050 and 12088101) and NSAF (Grant No. U1930403).

---

[1] R. Feynman, *Simulating physics with computers*, Int. J. Theor. Phys. **21**, 467 (1982).

[2] S. Lloyd, *Universal quantum simulators*, Science **273**, 1073 (1996).

[3] N. Metropolis and S. Ulam, *The Monte Carlo Method*, J. Am. Stat. Assoc. **44**, 335 (1949).

[4] B. J. Hammond, W. A. Lester, and P. J. Reynolds, *MonteCarlo Methods in ab Initio Quantum Chemistry*, (World Scientific, Singapore, 1994).

[5] M. Nightingale and C. Umrigar, *Quantum Monte Carlo Methods in Physics and Chemistry*, (Springer, New York, 1999).

[6] W. M. C. Foulkes, L. Mitas, R. J. Needs, and G. Rajagopal, *Quantum Monte Carlo simulations of solids*, Rev. Mod. Phys. **73**, 33 (2001).

[7] K. Schmidt and D. Ceperley, *The Monte Carlo Method in Condensed Matter Physics*, (Springer, Berlin, 1992).

[8] D. M. Ceperley, *Path integrals in the theory of condensed helium*, Rev. Mod. Phys. **67**, 279 (1995).

[9] J. Carlson, S.-Y. Chang, V. R. Pandharipande, and K. E. Schmidt, *Superfluid Fermi Gases with Large Scattering Length*, Phys. Rev. Lett. **91**, 050401 (2003).

[10] S. Giorgini, L. P. Pitaevskii, and S. Stringari, *Theory of ultracold atomic Fermi gases*, Rev. Mod. Phys. **80**, 1215 (2008).

[11] J. Carlson, S. Gandolfi, F. Pederiva, Steven C. Pieper, R. Schiavilla, K.E. Schmidt, and R.B. Wiringa, *Quantum Monte Carlo methods for nuclear physics*, Rev. Mod. Phys. **87**, 1067 (2015).

[12] J. Carlson, *Green's function Monte Carlo study of light nuclei*, Phys. Rev. C **36**, 2026 (1987).

[13] J. Carlson, *Alpha particle structure*, Phys. Rev. C **38**, 1879 (1988).

[14] R. Blankenbecler, D. J. Scalapino, and R. L. Sugar, *Monte Carlo calculations of coupled boson-fermion systems. I*, Phys. Rev. D **24**, 2278 (1981).

[15] K. E. Schmidt, and S. Fantoni, *A quantum Monte Carlo method for nucleon systems*, Phys. Lett. B **446**, 99 (1999).

[16] D. Lee, *Lattice simulations for few- and many-body systems*, Prog. Part. Nucl. Phys. **63**, 117 (2009).

[17] H. G. Evertz, G. Lana, and M. Marcu, *Cluster algorithm for vertex models*, Phys. Rev. Lett. **70**, 875 (1993).

[18] H. G. Evertz, *The Loop Algorithm*, Adv. Phys. **52**, 1 (2003).

[19] O. Syljuasen and A. W. Sandvik, *Quantum Monte Carlo with directed loops*, Phys. Rev. E **66**, 046701 (2002).

[20] S. Bour, D. Lee, H.-W. Hammer and Ulf-G. Meißner, *Ab initio Lattice Results for Fermi Polarons in Two Dimensions*, Phys. Rev. Lett. **115**, 185301 (2015).

[21] J. Lomnitz-Adler, V. Pandharipande, and R. Smith, *Monte Carlo calculations of triton and  $^4\text{He}$  nuclei with the Reid potential*, Nucl. Phys. A **361**, 399 (1981).

[22] J. Hubbard, *Electron correlations in narrow energy bands*, Proceedings of the Royal Society of London. Series A. Mathematical and Physical Sciences. **276**, 238257 (1963).

[23] M. Takahashi, *Half-filled Hubbard model at low temperature*, J. Phys. C: Solid State Phys. **10**, 1289 (1977).

[24] E. Wigner, *On the Consequences of the Symmetry of the Nuclear Hamiltonian on the Spectroscopy of Nuclei*, Phys. Rev. **51**, 106 (1937).

[25] B.-N. Lu, N. Li, S. Elhatisari, D. Lee, E. Epelbaum, Ulf-G. Meißner, *Essential elements for nuclear binding*, Phys. Lett. B **797**, 134863 (2019).

[26] D. Lee, S. Bogner, B. A. Brown, S. Elhatisari, E. Epelbaum, H. Hergert, M. Hjorth-Jensen, H. Krebs, N. Li, B.-N. Lu, Ulf-G. Meißner, *Hidden spin-isospin exchange symmetry*, arXiv:2010.09420.

[27] D. Hangleiter, I. Roth, D. Nagaj, and J. Eisert, *Easing the Monte Carlo sign problem*, Sci. Adv. **6**, eabb8341 (2020).

[28] G. Parisi, *On complex probabilities*, Phys. Lett. B **131**, 393 (1983).

[29] J. R. Klauder, *Stochastic Quantization*, Acta Phys. Austriaca Suppl. **25**, 251 (1983).

[30] M. Cristoforetti, F. D. Renzo, and L. Scorzato, *New approach to the sign problem in quantum field theories: High density QCD on a Lefschetz thimble*, Phys. Rev. D **86**, 074506 (2012).

[31] M. Cristoforetti, F. D. Renzo, A. Mukherjee, and L. Scorzato, *Monte Carlo simulations on the Lefschetz thimble: Taming the sign problem*, Phys. Rev. D **88**, 051501(R) (2013).

[32] J.-L. Wynen, E. Berkowitz, S. Krieg, T. Luu, and J. Ostheimer, *Machine learning to alleviate Hubbard-model sign problems*, Phys. Rev. B **103**, 125153 (2021).

[33] M. Troyer and U.-J. Wiese, *Computational Complexity and Fundamental Limitations to Fermionic Quantum Monte Carlo Simulations*, Phys. Rev. Lett. **94**, 170201 (2005).

[34] D. W. Berry, G. Ahokas, R. Cleve, B. C. Sanders, *Efficient quantum algorithms for simulating sparse Hamiltonians*, Commun. Math. Phys. **270**, 359 (2007).

[35] N. Wiebe, D. Berry, P. Hoyer, and B. C. Sanders, *Higher order decompositions of ordered operator exponentials*, J. Phys. A: Math. Theor. **43**, 065203 (2010).

[36] D. W. Berry, A. M. Childs, R. Cleve, R. Kothari, and R. D. Somma, *Simulating Hamiltonian dynamics with a truncated Taylor series*, Phys. Rev. Lett. **114**, 090502 (2015).

[37] R. Meister, S. C. Benjamin, and E. T. Campbell, *Tailoring Term Truncations for Electronic Structure Calculations Using a Linear Combination of Unitaries*, arXiv:2007.11624

[38] A. M. Childs and N. Wiebe, *Hamiltonian simulation using linear combinations of unitary operations*, Quantum Inf. Comput. **12**, 901 (2012).

[39] P. K. Faehrmann, M. Steudtner, R. Kueng, M. Kieferova, and J. Eisert, *Randomizing multi-product formulas for improved Hamiltonian simulation*, arXiv:2101.07808

[40] E. Campbell, *Random compiler for fast Hamiltonian simulation*, Phys. Rev. Lett. **123**, 070503 (2019).

[41] B. M. Terhal and D. P. DiVincenzo, *Problem of equilibration and the computation of correlation functions on a quantum computer*, Phys. Rev. A **61**, 022301 (2000).

[42] D. Bacon, A. M. Childs, I. L. Chuang, J. Kempe, D. W. Leung, and X. Zhou, *Universal simulation of Markovian quantum dynamics*, Phys. Rev. A **64**, 062302 (2001).

[43] M. Kliesch, T. Barthel, C. Gogolin, M. Kastoryano, and J. Eisert, *Dissipative quantum Church-Turing theorem*, Phys. Rev. Lett. **107**, 120501 (2011).

[44] H. Wang, S. Ashhab, and F. Nori, *Quantum algorithm for simulating the dynamics of an open quantum system*, Phys. Rev. A **83**, 062317 (2011).

[45] H.-Y. Su and Y. Li, *Quantum algorithm for the simulation of open-system dynamics and thermalization*, Phys. Rev. A **101**, 012328 (2020).

[46] D. Poulin and P. Wocjan *Sampling from the thermal quantum Gibbs state and evaluating partition functions with a quantum computer*, Phys. Rev. Lett. **103**, 220502 (2009).

[47] E. Bilgin and S. Boixo, *Preparing thermal states of quantum systems by dimension reduction*, Phys. Rev. Lett. **105**, 170405 (2010).

[48] K. Temme, T. J. Osborne, K. G. Vollbrecht, D. Poulin, and F. Verstraete, *Quantum Metropolis sampling*, Nature **471**, 87 (2011).

[49] A. Riera, C. Gogolin, and J. Eisert, *Thermalization in nature and on a quantum computer*, Phys. Rev. Lett. **108**, 080402 (2012).

[50] M.-H. Yung and A. Aspuru-Guzik, *A quantum-quantum Metropolis algorithm*, PNAS **109**, 754 (2012).

[51] D. Abrams and S. Lloyd, *Quantum algorithm providing exponential speed increase for finding eigenvalues and eigenvectors*, Phys. Rev. Lett. **83**, 5162 (1999).

[52] A. Aspuru-Guzik, A. D. Dutoi, P. J. Love, and M. Head-Gordon, *Simulated Quantum Computation of Molecular Energies*, Science **309**, 1704 (2005).

[53] T. E O'Brien, B. Tarasinski, and B. M. Terhal, *Quantum phase estimation of multiple eigenvalues for small-scale (noisy) experiments*, New J. Phys. **21**, 023022 (2019).

[54] R. D. Somma, *Quantum eigenvalue estimation via time series analysis*, New J. Phys. **21**, 123025 (2019).

[55] Y. Ge, J. Tura, and J. I. Cirac, *Faster ground state preparation and high-precision ground energy estimation with fewer qubits*, J. Math. Phys. **60**, 022202 (2019).

[56] A. E. Russo, K. M. Rudinger, B. C. A. Morrison, and A. D. Baczewski, *Evaluating Energy Differences on a Quantum Computer with Robust Phase Estimation*, Phys. Rev. Lett. **126**, 210501 (2021).

[57] S. Lu, M. C. Bañuls, and J. I. Cirac, *Algorithms for Quantum Simulation at Finite Energies*, PRX Quantum **2**, 020321 (2021).

[58] D. Wecker, B. Bauer, B. K. Clark, M. B. Hastings, and M. Troyer, *Gate-count estimates for performing quantum chemistry on small quantum computers*, Phys. Rev. A **90**, 022305 (2014).

[59] M. Reiher, N. Wiebe, K. M. Svore, D. Wecker, and M. Troyer, *Elucidating reaction mechanisms on quantum computers*, PNAS **114**, 7555 (2017).

[60] R. Babbush, C. Gidney, D. W. Berry, N. Wiebe, J. McClean, A. Paler, A. Fowler, and H. Neven, *Encoding Electronic Spectra in Quantum Circuits with Linear T Complexity*, Phys. Rev. X **8**, 041015 (2018).

[61] A. G. Fowler, M. Mariantoni, J. M. Martinis, and A. N. Cleland, *Surface codes: Towards practical large-scale quantum computation*, Phys. Rev. A **86**, 032324 (2012).

[62] B. Bauer, D. Wecker, A. J. Millis, M. B. Hastings, and M. Troyer, *Hybrid quantum-classical approach to correlated materials*, Phys. Rev. X **6**, 031045 (2016).

[63] A. Peruzzo, J. McClean, P. Shadbolt, M.-H. Yung, X.-Q. Zhou, P. J. Love, A. Aspuru-Guzik, and J. L. O’Brien, *A variational eigenvalue solver on a photonic quantum processor*, Nat. Commun. **5**, 4213 (2014).

[64] D. Wecker, M. B. Hastings, and M. Troyer, *Progress towards practical quantum variational algorithms*, Phys. Rev. A **92**, 042303 (2015).

[65] Y. Li and S. C. Benjamin, *Efficient variational quantum simulator incorporating active error minimisation*, Phys. Rev. X **7**, 021050 (2017).

[66] M. Otten, C. L. Cortes, and S. K. Gray, *Noise-Resilient Quantum Dynamics Using Symmetry-Preserving Ansatzes*, arXiv:1910.06284

[67] M. Benedetti, M. Fiorentini, and M. Lubasch, *Hardware-efficient variational quantum algorithms for time evolution*, arXiv:2009.12361

[68] S. Barison, F. Vicentini, and G. Carleo, *An efficient quantum algorithm for the time evolution of parameterized circuits*, arXiv:2101.04579

[69] J. W. Z. Lau, T. Haug, L. C. Kwek, and K. Bharti, *NISQ Algorithm for Hamiltonian Simulation via Truncated Taylor Series*, arXiv:2103.05500

[70] S. McArdle, T. Jones, S. Endo, Y. Li, S. C. Benjamin, and X. Yuan, *Variational ansatz-based quantum simulation of imaginary time evolution*, npj Quantum Inf. **5**, 75 (2019).

[71] M. Motta, C. Sun, A. T. K. Tan, M. J. O’Rourke, E. Ye, A. J. Minnich, F. G. S. L. Brandão, and G. Kim-Lic Chan, *Determining eigenstates and thermal states on a quantum computer using quantum imaginary time evolution*, Nat. Phys. **16**, 205 (2020).

[72] M. Suzuki, *Fractal decomposition of exponential operators with applications to many-body theories and Monte Carlo simulations*, Phys. Lett. A **146**, 319 (1990).

[73] H. Yoshida, *Construction of higher order symplectic integrators*, Phys. Lett. A **150**, 262 (1990).

[74] K. Temme, S. Bravyi, and J. M. Gambetta, *Error Mitigation for Short-Depth Quantum Circuits*, Phys. Rev. Lett. **119**, 180509 (2017).

[75] J. R. McClean, M. E. Kimchi-Schwartz, J. Carter, and W. A. de Jong, *Hybrid quantum-classical hierarchy for mitigation of decoherence and determination of excited states*, Phys. Rev. A **95**, 042308 (2017).

[76] S. Endo, S. Benjamin, and Y. Li, *Practical quantum error mitigation for near-future applications*, Phys. Rev. X **8**, 031027 (2018).

[77] T. A. Lähde, T. Luu, D. Lee, Ulf-G. Meißner, E. Epelbaum, H. Krebs, and G. Rupak, *Nuclear lattice simulations using symmetry-sign extrapolation*, Eur. Phys. J. A **51**, 92 (2015).

[78] E. Epelbaum, H. Krebs, T. A. Lähde, D. Lee, Ulf-G. Meißner, and G. Rupak, *Ab Initio Calculation of the Spectrum and Structure of  $^{16}\text{O}$* , Phys. Rev. Lett. **112**, 102501 (2014).

[79] G. Brassard, P. Hoyer, M. Mosca, and A. Tapp, *Quantum Amplitude Amplification and Estimation*, Quantum Computation and Quantum Information **305**, 53 (2002).

[80] S. McArdle, X. Yuan, and S. Benjamin, *Error-mitigated digital quantum simulation*, Phys. Rev. Lett. **122**, 180501 (2019).

[81] X. Bonet-Monroig, R. Sagastizabal, M. Singh, and T. E. O’Brien, *Low-cost error mitigation by symmetry verification*, Phys. Rev. A **98**, 062339 (2018).

[82] B. Koczor, *Exponential Error Suppression for Near-Term Quantum Devices*, arXiv:2011.05942

[83] W. J. Huggins, S. McArdle, T. E. O’Brien, J. Lee, N. C. Rubin, S. Boixo, K. B. Whaley, R. Babbush, and J. R. McClean, *Virtual Distillation for Quantum Error Mitigation*, arXiv:2011.07064

[84] P. Czarnik, A. Arrasmith, L. Cincio, and P. J. Coles, *Qubit-efficient exponential suppression of errors*, arXiv:2102.06056

[85] E. Knill, *Fault-Tolerant Postselected Quantum Computation: Threshold Analysis*, arXiv:quant-ph/0404104.

[86] J. J. Wallman and J. Emerson, *Noise Tailoring for Scalable Quantum Computation via Randomized Compiling*, Phys. Rev. A **94**, 052325 (2016).

[87] A. Strikis, D. Qin, Y. Chen, S.C. Benjamin, and Y. Li, *Learning-based quantum error mitigation*, arXiv:2005.07601

[88] P. Czarnik, A. Arrasmith, P. J. Coles, L. Cincio, *Error mitigation with Clifford quantum-circuit data*, arXiv:2005.10189

[89] T. E. O’Brien, S. Polla, N. C. Rubin, W. J. Huggins, S. McArdle, S. Boixo, J. R. McClean, and R. Babbush, *Error mitigation via verified phase estimation*, arXiv:2010.02538

[90] M. Huo and Y. Li, *Dual-state purification for practical quantum error mitigation*, arXiv:2105.01239

[91] T. Jones and S. Benjamin, *QuESTlink—Mathematica embiggened by a hardware-optimised quantum emulator*, Quantum Sci. Technol. **5**, 034012 (2020).

## Appendix A: Leading-order terms

Let  $A_j \equiv -ih_j\sigma_j\Delta t$  and  $A \equiv \sum_i A_i = -iH\Delta t$  for simplicity, the Taylor expansion of the time evolution operator reads

$$e^{-iH\Delta t} = e^A = \mathbb{1} + A + \frac{1}{2}A^2 + \frac{1}{6}A^3 + O(\Delta t^4). \quad (\text{A1})$$

We have

$$A^2 = \sum_{i < j} (A_i A_j + A_j A_i) + \sum_i A_i^2 \quad (\text{A2})$$

and

$$\begin{aligned} A^3 &= \sum_{i < j < k} (A_i A_j A_k + A_k A_j A_i + A_j A_i A_k \\ &\quad + A_k A_i A_j + A_i A_k A_j + A_j A_k A_i) \\ &\quad + \sum_{i < j} (A_i^2 A_j + A_j A_i^2 + A_i A_j A_i \\ &\quad + A_i A_j^2 + A_j^2 A_i + A_j A_i A_j) \\ &\quad + \sum_i A_i^3. \end{aligned} \quad (\text{A3})$$

### 1. First-order formula

According to the first-order formula, we have

$$\begin{aligned} S_1(\Delta t)^\dagger &= e^{-A_1} \cdots e^{-A_M} \\ &= \prod_{i=1}^M \left( \mathbb{1} - A_i + \frac{1}{2} A_i^2 - \frac{1}{6} A_i^3 + O(\Delta t^4) \right) \\ &= \mathbb{1} - A + \frac{1}{2} A^{(2)} - \frac{1}{6} A^{(3)} + O(\Delta t^4), \end{aligned} \quad (\text{A4})$$

where

$$A^{(2)} = 2 \sum_{i < j} A_i A_j + \sum_i A_i^2, \quad (\text{A5})$$

$$\begin{aligned} A^{(3)} &= 6 \sum_{i < j < k} A_i A_j A_k + 3 \sum_{i < j} (A_i^2 A_j + A_j A_i^2) \\ &\quad + \sum_i A_i^3. \end{aligned} \quad (\text{A6})$$

The correction operator is

$$\begin{aligned} V_1(\Delta t) &= \mathbb{1} - A^2 + \frac{1}{2} (A^2 + A^{(2)}) \\ &\quad + \frac{1}{2} A (A^{(2)} - A^2) + \frac{1}{6} (A^3 - A^{(3)}) \\ &\quad + O(\Delta t^4). \end{aligned} \quad (\text{A7})$$

Then, we have

$$\begin{aligned} F_1^{(2)}(\Delta t) &= -A^2 + \frac{1}{2} (A^2 + A^{(2)}) = \frac{1}{2} (A^{(2)} - A^2) \\ &= \frac{1}{2} \sum_{i < j} (A_i A_j - A_j A_i) \end{aligned} \quad (\text{A8})$$

and

$$\begin{aligned} F_1^{(3)}(\Delta t) &= \frac{1}{2} A (A^{(2)} - A^2) + \frac{1}{6} (A^3 - A^{(3)}) \\ &= \frac{1}{2} \sum_{i < j < k} (A_i A_j A_k - A_k A_j A_i + A_j A_i A_k \\ &\quad + A_k A_i A_j - A_i A_k A_j - A_j A_k A_i) \\ &\quad + \frac{1}{2} \sum_{i < j} (A_i^2 A_j - A_i A_j A_i - A_j^2 A_i + A_j A_i A_j) \\ &\quad + \frac{1}{6} (A^3 - A^{(3)}) \\ &= \frac{1}{6} \sum_{i < j < k} (-2 A_i A_j A_k - 2 A_k A_j A_i + 4 A_j A_i A_k \\ &\quad + 4 A_k A_i A_j - 2 A_i A_k A_j - 2 A_j A_k A_i) \\ &\quad + \frac{1}{6} \sum_{i < j} (A_i^2 A_j + A_j A_i^2 - 2 A_i A_j A_i \\ &\quad - 2 A_i A_j^2 - 2 A_j^2 A_i + 4 A_j A_i A_j). \end{aligned} \quad (\text{A9})$$

According to Eq. (A8), the contribution of  $F_1^{(2)}(\Delta t)$  to the normalisation factor is

$$\sum_{i < j} |h_i h_j| \Delta t^2 < \frac{1}{2} \left( \sum_i |h_i| \right)^2 \Delta t^2. \quad (\text{A10})$$

### 2. Second-order formula

We can write the second-order correction operator as

$$\begin{aligned} V_2(\Delta t) &= V_1\left(-\frac{\Delta t}{2}\right)^\dagger V_1\left(\frac{\Delta t}{2}\right) \\ &= \mathbb{1} + F_1^{(3)}\left(\frac{\Delta t}{2}\right) + F_1^{(3)}\left(-\frac{\Delta t}{2}\right)^\dagger \\ &\quad + O(\Delta t^5). \end{aligned} \quad (\text{A11})$$

Then, we have

$$F_2^{(3)}(\Delta t) = F_1^{(3)}\left(\frac{\Delta t}{2}\right) + F_1^{(3)}\left(-\frac{\Delta t}{2}\right)^\dagger. \quad (\text{A12})$$

Accordingly, the contribution of  $F_2^{(3)}(\Delta t)$  to the normalisation factor is

$$\begin{aligned} &\frac{1}{3} \sum_{i < j < k} |h_i h_j h_k| \Delta t^3 + \frac{1}{12} \sum_{i < j} (|h_i^2 h_j| + 2|h_i h_j^2|) \Delta t^3 \\ &< \frac{1}{18} \left( \sum_i |h_i| \right)^3 \Delta t^3. \end{aligned} \quad (\text{A13})$$

## Appendix B: Fermi-Hubbard model

The Hamiltonian of Fermi-Hubbard model reads

$$\begin{aligned} H_{\text{FH}} &= - \sum_{i < j} J_{i,j} \sum_{s=\uparrow,\downarrow} (c_{i,s}^\dagger c_{j,s} + c_{j,s}^\dagger c_{i,s}) \\ &\quad + U \sum_i \left( c_{i,\uparrow}^\dagger c_{i,\uparrow} - \frac{\mathbb{1}}{2} \right) \left( c_{i,\downarrow}^\dagger c_{i,\downarrow} - \frac{\mathbb{1}}{2} \right), \end{aligned} \quad (\text{B1})$$

where  $c_{i,s}$  is the annihilation operator for the fermion with spin- $s$  on the  $i$ th site. Operators of fermions satisfy  $\{c_{i,s}, c_{i',s'}\} = 0$  and  $\{c_{i,s}, c_{i',s'}^\dagger\} = \delta_{i,i'}\delta_{s,s'}\mathbb{1}$ . Here, we have modified the original Fermi-Hubbard model by adding a uniform on-site potential  $-\frac{U}{2}N$ , which does not affect the time evolution if the initial state is an eigenstate of the total particle number operator  $N = \sum_{i,s} c_{i,s}^\dagger c_{i,s}$ . For a bipartite lattice,  $J_{i,j} = 0$  for all  $i + j \in \text{Even}$ , i.e. two sites are not coupled if their labels have the same parity.

To encode the Fermi-Hubbard model into qubits, we take the Jordan-Wigner transformation

$$\begin{aligned} c_{i,\uparrow} &= \frac{Y_{2i-1} - iZ_{2i-1}}{2} \prod_{l < 2i-1} X_l, \\ c_{i,\downarrow} &= \frac{Y_{2i} - iZ_{2i}}{2} \prod_{l < 2i} X_l, \end{aligned} \quad (\text{B2})$$

where  $X_a, Y_a, Z_a$  are Pauli operators of the qubit- $a$ . The spin- $\uparrow$  and spin- $\downarrow$  on the  $i$ th site are encoded on the qubit- $(2i-1)$  and qubit- $2i$ , respectively. According to the Jordan-Wigner transformation, the qubit Hamiltonian of Fermi-Hubbard model is

$$\begin{aligned} H_{\text{FH}} &= - \sum_{i < j} \frac{J_{i,j}}{2} (Y_{2i-1,2j-1} + Z_{2i-1,2j-1} \\ &\quad + Y_{2i,2j} + Z_{2i,2j}) + \frac{U}{4} \sum_i X_{2i-1} X_{2i}, \end{aligned} \quad (\text{B3})$$

where

$$\begin{aligned} Y_{a,b} &= Y_a Y_b \prod_{a < l < b} X_l, \\ Z_{a,b} &= Z_a Z_b \prod_{a < l < b} X_l. \end{aligned} \quad (\text{B4})$$

Each Pauli operator  $\sigma$  corresponds to an  $x$  binary string according to Eq. (44), and we define  $\mathbf{x}(\sigma) \equiv (x_1, \dots, x_n)$  is the  $x$  binary string of the Pauli operator  $\sigma$ . A Hamiltonian does not have short-time interference if  $\mathbf{x}(\sigma_1) \neq \mathbf{x}(\sigma_2)$  for any pair of Pauli-operator terms  $\sigma_1$  and  $\sigma_2$  in the Hamiltonian. We use  $\mathbf{x}_{a,b}$  to denote the binary string that  $x_k = 0$  if  $k < a$  or  $k > b$  and  $x_k = 1$  if  $a \leq k \leq b$ . Then,

$$\begin{aligned} \mathbf{x}(Y_{a,b}) &= \mathbf{x}_{a,b}, \\ \mathbf{x}(Z_{a,b}) &= \mathbf{x}_{a+1,b-1}, \\ \mathbf{x}(X_{2i-1}X_{2i}) &= \mathbf{x}_{2i-1,2i}. \end{aligned} \quad (\text{B5})$$

We can find that  $x$  strings of  $Y_{a,b}$  and  $Z_{a,b}$  terms in Eq. (B3) are all different from  $X_{2i-1}X_{2i}$  terms, note that  $a$  and  $b$  have the same parity. The only question is whether  $Y_{a,b}$  and  $Z_{a',b'}$  have the same  $x$  string. If their  $x$  strings are the same, we must have  $a = a' + 1$  and  $b = b' - 1$ . For a bipartite lattice,  $\frac{b-a}{2}$  and  $\frac{b'-a'}{2}$  are both odd, however,  $\frac{b'-1-a'-1}{2}$  is even if  $\frac{b'-a'}{2}$  is odd. Therefore,  $x$  strings of  $Y_{a,b}$  and  $Z_{a',b'}$  are always different.